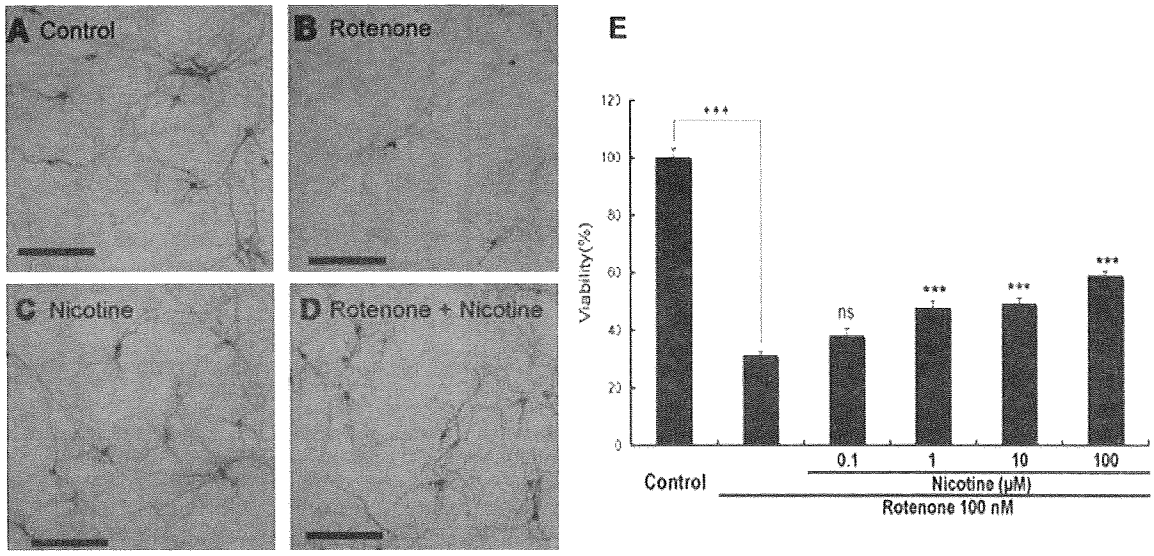

Fig. 6. Effect of nicotine on TH-positive neurons. Nicotine showed dose-dependent neuroprotection for dopaminergic neurons. A–D: Representative findings of each group of dopaminergic neurons. **A:** Control. **B:** Rotenone 100 nM. **C:** Nicotine 100 μM. **D:** Rotenone and nicotine added simultaneously for 48 hr. Scale bar = 200 μm. **E:** Statistical analysis of the viability of TH-positive cells, standardized by the number of control. Each value is the mean ± SEM, $n = 8$, $^{***}P < 0.001$ vs. rotenone 100 nM, $^{+++}P < 0.001$.

(Cormier et al., 2003), as well as about 6-OHDA models (Visanji et al., 2006). Our orally rotenone-treated mouse model showed motor deficits, dopaminergic cell death in the substantia nigra, nerve terminal/axonal loss in the striatum. These findings are relevant to some previous reports about rotenone PD models (Schmidt and Alam, 2006; Ravenstijn et al., 2008). However, some failed to make animal PD models by rotenone (Lapointe et al., 2004; Höglinger et al., 2006). Although the mechanism is unclear, these inconsistencies may arise from the differences in animal species or mode of compound delivery (Quik et al., 2007b). Our data suggest that nicotinic protection might be more remarkable in cell bodies than in axon or nerve terminals. That was relevant to the previous reports about paraquat-induced (Khwaja et al., 2007) or MPTP-induced (Parain et al., 2003) mouse models, both mitochondrial complex I inhibitors, and rotarod treadmill test was reported to be useful for evaluating motor deficits in MPTP-treated mouse models of parkinsonism (Rozas et al., 1998).

The present data showed nicotinic neuroprotection was via nAChRs, and RT-PCR suggested that both α7 and α4β2 nAChRs expressed on rat mesencephalic cells, whether they were on neurons or not. A previous report about the protective effect of nicotine against neurotoxicity suggested that a non-α7 receptor was involved (Jeyarasasingam et al., 2002). Our data showed that both α7 and α4β2 receptors had relationships with neuroprotection. We have previously shown that neuronal α7 nAChR stimulation appeared to activate the PI3K-Akt/PKB pathway or pathways, leading to induced expression of antiapoptotic B cell lymphoma protein–mediating neuronal survival in Aβ-potentiated glutamate-induced neurotoxicity (Kihara et al., 2001). On the other hand, neuronal α4β2 nAChR stimulation causes DA release (Champtiaux et al., 2003), and our data showed the neuroprotective effect also occurred via α4β2 nAChRs, so the mechanism of neuroprotection could vary for different receptor subclasses. In addition, we have also shown the protective effect of dopamine D2 receptor agonists in cortical neurons via the PI3K cascade (Kihara et al., 2002). Also other nAChR subclasses were reported to be protective (Visanji et al., 2006), and nAChR agonists were protective. Previously it was reported that α4β2 nAChR stimulation might improve behavior of PD models (O'Neill et al., 2002), and epibatidine protected bovine chromaffin cells against rotenone-induced toxicity (Egea et al., 2007). We could not examine the effect of α6β2 nAChR stimulation, but it was reported to be neuroprotective (Quik and McIntosh, 2006). Further studies should be needed to assess other nAChRs by using other nAChR agonists or nicotinic components.

Our primary cultures contained not only neuronal cells but also glial cells, so glial cells may also be partly responsible for nicotinic neuroprotection. Microglial cells have α7 nAChRs whose stimulation reduced the release of cytotoxic cytokines such as TNFα (Suzuki et al., 2006) and then decreased the activity of neuronal NF-κB (Liu et al., 2007). Chronically nicotine-treated rats might have NGF up-regulation in astrocytes of the

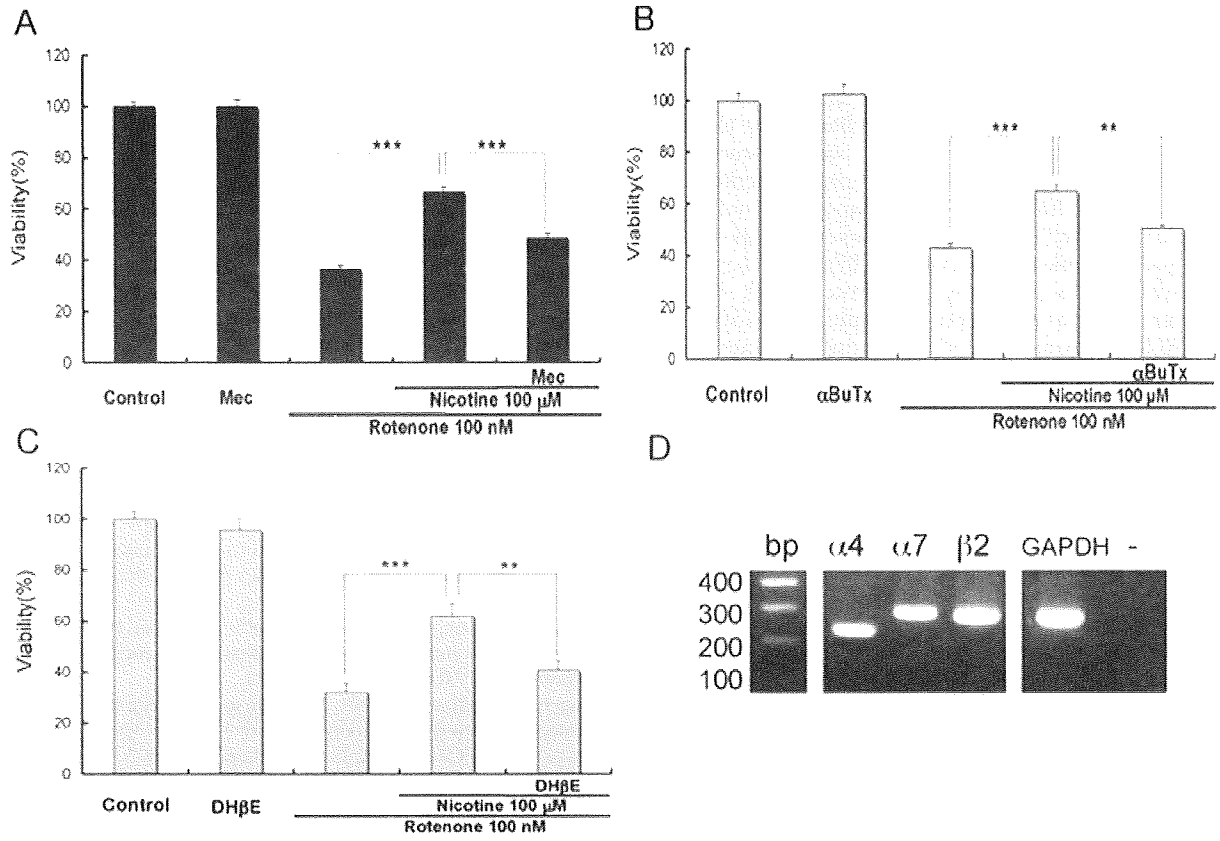

Fig. 7. A–C: Simultaneous administration of nicotinic acetylcholine receptor (nAChR) antagonists. Each antagonist blocked nicotinic neuroprotection, so it was suggested receptor-mediated. **A:** Mec, mecamylamine 100 μM, a broad-spectrum antagonist of nAChRs. **B:** αBuTx, α-bungarotoxin 100 nM, an α7 nAChR antagonist. **C:** DHβE, dihydro-β-erythroidine 1 μM, an α4β2 nAChR antagonist. Each value is the mean ± SEM, $n = 8$, $^{**}P < 0.01$, $^{***}P < 0.001$. **D:** Representative expression of mRNA for subunits of nAChRs in cultures of rat mesencephalic cells (day 8), RT-PCR products on an ethidium-bromide-stained gel. bp, number of base pairs; GAPDH, glyceraldehyde-3-phosphate dehydrogenase, which served as the internal control; −, negative control. Expression of mRNA for each α4,α7 and β2 subunit was remarkable. Paired primers used were indicated in Table I. The same results were obtained three times.

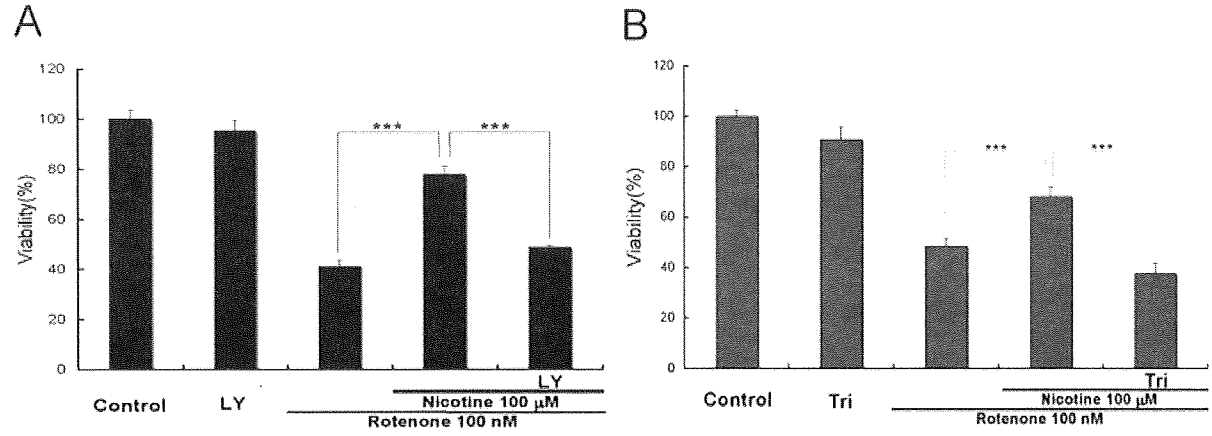

Fig. 8. Effects of the inhibitors of the PI3K-Akt/PKB pathway. Inhibition of either PI3K or Akt/PKB suppressed neuroprotective effect of nicotine. **A:** LY, LY294002 10 μM, an inhibitor of PI3K. **B:** Tri, triciribine 1 μM, an inhibitor of Akt/PKB. Each value is the mean ± SEM, $n = 8$, $^{***}P < 0.001$.

frontoparietal cortex (Martínez-Rodríguez et al., 2003). Nicotine decreased the number of activated microglial cells and TNFα and then protected dopaminergic neurons of MPTP-treated mice (Park et al., 2007). So glial cells may also play a role for the mechanism of the neuroprotection we have seen in the present study. We should also analyze glial neuroprotection by nicotine.

As mentioned above, other compounds that stimulate nAChRs show functional improvement in nonhuman primates (Quik et al., 2006, 2007a) and have neuroprotective effects are now on clinical trial, but the results were controversial. For example, SIB-1508Y, an α4β2 nAChR agonist, failed to improve symptoms of PD (Parkinson Study Group, 2006). Some cholinesterase inhibitors, for example, galantamine is an allosteric potentiating ligand (Santos et al., 2002) and stimulates cholinergic neurons in the nucleus basalis of Meynert, were reported to be effective for cognitive dysfunction of PD with dementia and Lewy body disease, a parkinsonism with hallucination and fluctuating dementia (Burn et al., 2006; Mentis et al., 2006, Miyasaki et al., 2006), but there may be deterioration of motor dysfunction due to simultaneous muscarinic acetylcholine receptor stimulation in the striatum. Thus, further analysis of glial neuroprotective effect by nicotine may be needed.

In conclusion, by stimulating nAChRs, the PI3K-Akt/PKB pathway or pathways could be activated to suppress dopaminergic cell death induced by rotenone. Additionally, chronic oral administration of rotenone induced motor deficits and nigrostriatal dopaminergic neurodegeneration in C57/BL6 mice, and nicotine attenuated both of them. These results suggest that derivatives of nicotine or agents that stimulate nAChRs may be useful for neuroprotective therapies targeting PD. In addition, rotenone-treated mice may be useful for understanding the mechanisms of dopaminergic cell death and may serve as a model of environmental factors involved in PD pathogenesis.

ACKNOWLEDGMENTS

This work was supported in part by the 21st Century Center of Excellence (COE) Program, the grants from Ministry of Education, Culture, Sports, Science and Technology of Japan, Japan Society for the Promotion of Science, Ministry of Health, Labour and Welfare of Japan, Smoking Research Foundation, and Philip Morris USA Inc. and Philip Morris International.

We thank to Megumi Asada-Utsugi, School of Health Sciences, Faculty of Medicine, Kyoto University, for contributing to the RT-PCR analysis.

REFERENCES

Akaike A, Tamura Y, Yokota T, Shimohama S, Kimura J. 1994. Nicotine-induced protection of cultured cortical neurons against N-methyl-D-aspartate receptor–mediated glutamate cytotoxicity. Brain Res 644:181–187.

Baquet Z, Bickford P, Jones K. 2005. Brain-derived neurotrophic factor is required for the establishment of the proper number of dopaminergic neurons in the substantia nigra pars compacta. J Neurosci 25:6251–6259.

Betarbet R, Sherer T, MacKenzie G, Garcia-Osuna M, Panov A, Greenamyre J. 2000. Chronic systemic pesticide exposure reproduces features of Parkinson's disease. Nat Neurosci 3:1301–1306.

Burn D, Emre M, McKeith I, De Deyn P, Aarsland D, Hsu C, Lane R. 2006. Effects of rivastigmine in patients with and without visual hallucinations in dementia associated with Parkinson's disease. Mov Disord 21:1899–1907.

Champtiaux N, Gotti C, Cordero-Erausquin M.David D, Przybylski C, Léna C, Clementi F, Moretti M, Rossi F, Le Novère N, McIntosh J, Gardier A, Changeux J. 2003. Subunit composition of functional nicotinic receptors in dopaminergic neurons investigated with knock-out mice. J Neurosci 23:7820–7829.

Chomczynski P, Sacchi N. 1987. Single-step method of RNA isolation by acid guanidinium thiocyanate-phenol-chloroform extraction. Anal Biochem 162:156–159.

Cormier A, Morin C, Zini R, Tillement J, Lagrue G. 2003. Nicotine protects rat brain mitochondria against experimental injuries. Neuropharmacology 44:642–652.

De Reuck J, De Weweire M, Van Maele G, Santens P. 2005. Comparison of age of onset and development of motor complications between smokers and non-smokers in Parkinson's disease. J Neurol Sci 231:35–39.

Du F, Li R, Huang Y, Li X, Le W. 2005. Dopamine D3 receptor-preferring agonists induce neurotrophic effects on mesencephalic dopamine neurons. Eur J Neurosci 22:2422–2430.

Dunnett S, Björklund A. 1999. Prospects for new restorative and neuroprotective treatments in Parkinson's disease. Nature 399:A32–A39.

Egea J, Rosa A, Cuadrado A, García A, López M. 2007. Nicotinic receptor activation by epibatidine induces heme oxygenase-1 and protects chromaffin cells against oxidative stress. J Neurochem 102:1842–1852.

Fujita M, Ichise M, Zoghbi S, Liow J, Ghose S, Vines D, Sangare J, Lu J, Cropley V, Iida H, Kim K, Cohen R, Bara-Jimenez W, Ravina B, Innis R. 2006. Widespread decrease of nicotinic acetylcholine receptors in Parkinson's disease. Ann Neurol 59:174–177.

Grinevich V, Letchworth S, Lindenberger K, Menager J, Mary V, Sadieva K, Buhlman L, Bohme G, Pradier L, Benavides J, Lukas R, Bencherif M. 2005. Heterologous expression of human α6β4β3α5 nicotinic acetylcholine receptors: binding properties consistent with their natural expression require quaternary subunit assembly including the α5 subunit. J Pharmacol Exp Ther 312:619–626.

Gundersen H, Bendtsen T, Korbo L, Marcussen N, Møller A, Nielsen K, Nyengaard J, Pakkenberg B, Sørensen F, Vesterby A. 1988. Some new, simple and efficient stereological methods and their use in pathological research and diagnosis. APMIS 96:379–394.

Höglinger G, Oertel W, Hirsch E. 2006. The rotenone model of parkinsonism—the five years inspection. J Neural Transm Suppl 70:269–272.

Inden M, Kitamura Y, Takeuchi H, Yanagida T, Takata K, Kobayashi Y, Taniguchi T, Yoshimoto K, Kaneko M, Okuma Y, Taira T, Ariga H, Shimohama S. 2007. Neurodegeneration of mouse nigrostriatal dopaminergic system induced by repeated oral administration of rotenone is prevented by 4-phenylbutyrate, a chemical chaperone. J Neurochem 101:1491–1504.

Iravani M, Haddon C, Cooper J, Jenner P, Schapira A. 2006. Pramipexole protects against MPTP toxicity in non-human primates. J Neurochem 96:1315–1321.

Jeyarasasingam G, Tompkins L, Quik M. 2002. Stimulation of non-α7 nicotinic receptors partially protects dopaminergic neurons from 1-methyl-4-phenylpyridinium-induced toxicity in culture. Neuroscience 109:275–285.

Kagitani F, Uchida S, Hotta H, Sato A. 2000. Effects of nicotine on blood flow and delayed neuronal death following intermittent transient ischemia in rat hippocampus. Jpn J Physiol 50:585–595.

Khwaja M, McCormack A, McIntosh J, Di Monte D, Quik M. 2007. Nicotine partially protects against paraquat-induced nigrostriatal damage in mice; link to alpha6beta2* nAChRs. J Neurochem 100:180–190.

Kihara T, Shimohama S, Sawada H, Kimura J, Kume T, Kochiyama H, Maeda T, Akaike A. 1997. Nicotinic receptor stimulation protects neurons against beta-amyloid toxicity. Ann Neurol 42:159–163.

Kihara T, Shimohama S, Sawada H, Honda K, Nakamizo T, Shibasaki H, Kume T, Akaike A. 2001. α7 nicotinic receptor transduces signals to phosphatidylinositol 3-kinase to block Abeta-amyloid-induced neurotoxicity. J Biol Chem 276:13541–13546.

Kihara T, Shimohama S, Sawada H, Honda K, Nakamizo T, Kanki R, Yamashita H, Akaike A. 2002. Protective effect of dopamine D2 agonists in cortical neurons via the phosphatidylinositol 3 kinase cascade. J Neurosci Res 70:274–282.

Lapointe N, St-Hilaire M, Martinoli M, Blanchet J, Gould P, Rouillard C, Cicchetti F. 2004. Rotenone induces non-specific central nervous system and systemic toxicity. FASEB J 18:717–719.

Liu Q, Zhang J, Zhu H, Qin C, Chen Q, Zhao B. 2007. Dissecting the signaling pathway of nicotine-mediated neuroprotection in a mouse Alzheimer disease model. FASEB J 21:61–73.

Martínez-Rodríguez R, Toledano A, Alvarez M, Turégano L, Colman O, Rosés P, Gómez de Segura I, De Miguel E. 2003. Chronic nicotine administration increases NGF-like immunoreactivity in frontoparietal cerebral cortex. J Neurosci Res 73:708–716.

Mann V, Cooper J, Krige D, Daniel S, Schapira A, Marsden C. 1992. Brain, skeletal muscle and platelet homogenate mitochondrial function in Parkinson's disease. Brain 115(Pt 2):333–342.

Mentis M, Delalot D, Naqvi H, Gordon M, Gudesblatt M, Edwards C, Donatelli L, Dhawan V, Eidelberg D. 2006. Anticholinesterase effect on motor kinematic measures and brain activation in Parkinson's disease. Mov Disord 21:549–555.

Miyasaki J, Shannon K, Voon V, Ravina B, Kleiner-Fisman G, Anderson K, Shulman L, Gronseth G, Weiner W;Quality Standards Subcommittee of the American Academy of Neurology. 2006. Practice Parameter: evaluation and treatment of depression, psychosis, and dementia in Parkinson disease (an evidence-based review): report of the Quality Standards Subcommittee of the American Academy of Neurology. Neurology 66:996–1002.

Mizuno Y, Yoshino H, Ikebe S, Hattori N, Kobayashi T, Shimoda-Matsubayashi S, Matsumine H, Kondo T. 1998. Mitochondrial dysfunction in Parkinson's disease. Ann Neurol 44(3 Suppl 1):S99–S109.

Morens D, Grandinetti A, Reed D, White L, Ross G. 1995. Cigarette smoking and protection from Parkinson's disease: false association or etiologic clue? Neurology 45:1041–1051.

Nakamizo T, Kawamata J, Yamashita H, Kanki R, Kihara T, Sawada H, Akaike A, Shimohama S. 2005. Stimulation of nicotinic acetylcholine receptors protects motor neurons. Biochem Biophys Res Commun 330:1285–1289.

O'Neill M, Murray T, Lakies V, Visanji N, Duty S. 2002. The role of neuronal nicotinic acetylcholine receptors in acute and chronic neurodegeneration. Curr Drug Targets CNS Neurol Disord 1:399–411.

Parain K, Hapdey C, Rousselet E, Marchand V, Dumery B, Hirsch E. 2003. Cigarette smoke and nicotine protect dopaminergic neurons against the 1-methyl-4-phenyl-1,2,3,6-tetrahydropyridine Parkinsonian toxin. Brain Res 984:224–232.

Park H, Lee P, Ahn Y, Choi Y, Lee G, Lee D, Chung E, Jin B. 2007. Neuroprotective effect of nicotine on dopaminergic neurons by anti-inflammatory action. Eur J Neurosci 26:79–89.

Parker W Jr, Boyson S, Parks J. 1989. Abnormalities of the electron transport chain in idiopathic Parkinson's disease. Ann Neurol 26:719–723.

Parkinson Study Group. 2006. Randomized placebo-controlled study of the nicotinic agonist SIB-1508Y in Parkinson disease. Neurology 66:408–410.

Quik M. 2004. Smoking, nicotine and Parkinson's disease. Trends Neurosci 27:561–568.

Quik M, McIntosh J. 2006. Striatal alpha6* nicotinic acetylcholine receptors: potential targets for Parkinson's disease therapy. J Pharmacol Exp Ther 316:481–489.

Quik M, Chen L, Parameswaran N, Xie X, Langston J, McCallum S. 2006. Chronic oral nicotine normalizes dopaminergic function and synaptic plasticity in 1-methyl-4-phenyl-1,2,3,6- tetrahydropyridine-lesioned primates. J Neurosci 26:4681–4689.

Quik M, Cox H, Parameswaran N, O'Leary K, Langston J, Di Monte D. 2007a. Nicotine reduces levodopa-induced dyskinesias in lesioned monkeys. Ann Neurol 62:588–596.

Quik M, O'Neill M, Perez X. 2007b. Nicotine neuroprotection against nigrostriatal damage: importance of the animal model. Trends Pharmacol Sci 28:229–235.

Ravenstijn P, Merlini M, Hameetman M, Murray T, Ward M, Lewis H, Ball G, Mottart C, de Ville de Goyet C, Lemarchand T, van Belle K, O'Neill M, Danhof M, de Lange E. 2008. The exploration of rotenone as a toxin for inducing Parkinson's disease in rats, for application in BBB transport and PK-PD experiments. J Pharmacol Toxicol Methods 57:114–130.

Rozas G, Liste I, Guerra M, Labandeira-Garcia J. 1998. Sprouting of the serotonergic afferents into striatum after selective lesion of the dopaminergic system by MPTP in adult mice. Neurosci Lett 245:151–154.

Santos M, Alkondon M, Pereira E, Aracava Y, Eisenberg H, Maelicke A, Albuquerque E. 2002. The nicotinic allosteric potentiating ligand galantamine facilitates synaptic transmission in the mammalian central nervous system. Mol Pharmacol 61:1222–1234.

Sawada H, Kohno R, Kihara T, Izumi Y, Sakka N, Ibi M, Nakanishi M, Nakamizo T, Yamakawa K, Shibasaki H, Yamamoto N, Akaike A, Inden M, Kitamura Y, Taniguchi T, Shimohama S. 2004. Proteasome mediates dopaminergic neuronal degeneration, and its inhibition causes alpha-synuclein inclusions. J Biol Chem 279:10710–10719.

Schapira A. 2006. Etiology of Parkinson's disease. Neurology 66(10 Suppl 4):S10–S23.

Schmidt W, Alam M. 2006. Controversies on new animal models of Parkinson's disease pro and con: the rotenone model of Parkinson's disease (PD). J Neural Transm Suppl 70:273–276.

Shimohama S, Greenwald D, Shafron D, Akaike A, Maeda T, Kaneko S, Kimura J, Simpkins C, Day A, Meyer E. 1998. Nicotinic α7 receptors protect against glutamate neurotoxicity and neuronal ischemic damage. Brain Res 779:359–363.

Shimohama S, Sawada H, Kitamura Y, Taniguchi T. 2003. Disease model: Parkinson's disease. Trends Mol Med 9:360–365.

Suzuki T, Hide I, Matsubara A, Hama C, Harada K, Miyano K, Andrä M, Matsubayashi H, Sakai N, Kohsaka S, Inoue K, Nakata Y. 2006. Microglial α7 nicotinic acetylcholine receptors drive a phospholipase C/IP3 pathway and modulate the cell activation toward a neuroprotective role. J Neurosci Res 83:1461–1470.

Visanji N, O'Neill M, Duty S. 2006. Nicotine, but neither the alpha4-beta2 ligand RJR2403 nor an alpha7 nAChR subtype selective agonist, protects against a partial 6-hydroxydopamine lesion of the rat median forebrain bundle. Neuropharmacology 51:506–516.

West M, Slomianka L, Gundersen J. 1991. Unbiased stereological estimation of the total number of neurons in the subdivisions of the rat hippocampus using the optical fractionator. Anat Rec 231:482–497.

Wirdefeldt K, Gatz M, Pawitan Y, Pedersen N. 2005. Risk and protective factors for Parkinson's disease: a study in Swedish twins. Ann Neurol 57:27–33.

Xie Y, Bezard E, Zhao B. 2005. Investigating the receptor-independent neuroprotective mechanisms of nicotine in mitochondria. J Biol Chem 280:32405–32412.

Neuroscience Research 66 (2010) 151–161

Contents lists available at ScienceDirect

Neuroscience Research

journal homepage: www.elsevier.com/locate/neures

Loss of PINK1 in medaka fish (*Oryzias latipes*) causes late-onset decrease in spontaneous movement

Hideaki Matsui [a,b], Yoshihito Taniguchi [b,c], Haruhisa Inoue [a,b], Yoshito Kobayashi [a], Yoshiyuki Sakaki [d,1], Atsushi Toyoda [d,2], Kengo Uemura [a,b], Daisuke Kobayashi [e], Shunichi Takeda [b,c,*], Ryosuke Takahashi [a,b,**]

[a] Department of Neurology, Kyoto University, Graduate School of Medicine, 54 Shogoin-Kawahara-cho, Sakyo-ku, Kyoto 606-8507, Japan
[b] Core Research for Evolutional Science and Technology (CREST), Japan Science and Technology Agency, Japan
[c] Department of Radiation Genetics, Kyoto University, Graduate School of Medicine, Yoshida-Konoe-cho, Sakyo-ku, Kyoto 606-8501, Japan
[d] RIKEN Genomic Sciences Center, Yokohama 230-0045, Japan
[e] Department of Anatomy and Developmental Biology, Kyoto Prefectural University of Medicine, Kyoto 602-0841, Japan

ARTICLE INFO

Article history:
Received 21 May 2009
Received in revised form 16 October 2009
Accepted 23 October 2009
Available online 4 November 2009

Keywords:
Parkinson's disease
PTEN-induced kinase 1 (*PINK1*)
Medaka fish (*Oryzias latipes*)
TILLING (targeted induced local lesions in genomes)
Dopamine
Movement disorder

ABSTRACT

Parkinson's disease is a neurodegenerative disease associated with the degeneration of dopaminergic neurons in the substantia nigra. The PTEN-induced kinase 1 gene (*PINK1*) is responsible for recessive inherited familial Parkinson's disease (PARK6). Neither the function of PINK1 nor its role in the prevention of Parkinson's disease is fully understood. Gene disruption of *PINK1* causes remarkably different phenotypes in animal models such as *Drosophila melanogaster*, zebrafish, and mouse, none of which recapitulate Parkinson's-disease-like symptoms. We established *PINK1*-gene-disrupted medaka fish. These mutant fish grew normally at first, then developed significant decrease in the frequency of spontaneous swimming movements in the late-adult stage. Although the mutants did not show any dopaminergic cell loss, the amount of 3,4-dihydroxyphenylacetic acid, a major metabolite of dopamine, decreased. Thus, PINK1 contributes to the maintenance of dopamine metabolism, even before the selective death of dopaminergic neurons. Our animal model is therefore a valuable tool to detect pathogenesis in Parkinson's patients in the early stages.

1. Introduction

Parkinson's disease (PD) is the second-most common neurodegenerative disease among humans. It is associated with the degeneration of dopaminergic neurons in a subset of neuronal populations represented by the substantia nigra pars compacta in the midbrain. Although the majority of cases develop sporadically, 5–10% of PD patients are familial, with the disease caused by gene mutation (Gasser, 2005). To date, 10 different genes responsible for familial PD have been identified. The functional analysis of these genes is important to our understanding of the molecular pathogenesis of PD. Recessive inherited familial PD (PARK6) is attributable to mutations in the *PINK1* gene (Valente et al., 2004). These mutations appear to compromise the function of the PINK1 protein (Sim et al., 2006).

PINK1 is a highly conserved 581 amino acid protein. The gene is ubiquitously expressed in the human brain (Gandhi et al., 2006) and seems to be activated by a tumor suppressor, PTEN (Unoki and Nakamura, 2001). The *PINK1* gene encodes a kinase and contains a mitochondria-targeting motif. One of the putative substrates of the kinase is TNF receptor-associated protein 1 (TRAP1), though its biological significance remains elusive (Pridgeon et al., 2007). PINK1 plays a protective role against oxidative stress and MPTP (Wood-Kaczmar et al., 2008; Haque et al., 2008). Silencing of the *PINK1* gene results in mitochondrial pathology in the human cell line (Exner et al., 2007).

Gene disruption of *PINK1* causes distinctly different phenotypes in different animal models. Mice deficient in PINK1 exhibit impaired dopamine release, but not movement disorders or dopaminergic cell death (Kitada et al., 2007). Loss of PINK1 function in *Drosophila melanogaster* results in a drastic phenotype that includes male sterility and the degeneration of both muscle and dopaminergic neurons with massive mitochondria-related pathology (Clark et al., 2006; Park et al., 2006; Yang et al., 2006). In

* Corresponding author at: Department of Radiation Genetics, Kyoto University, Graduate School of Medicine, Yoshida-Konoe-cho, Sakyo-ku, Kyoto 606-8501, Japan.
** Corresponding author at: Department of Neurology, Kyoto University, Graduate School of Medicine, 54 Shogoin-Kawahara-cho, Sakyo-ku, Kyoto 606-8507, Japan.
E-mail addresses: stakeda@rg.med.kyoto-u.ac.jp (S. Takeda), ryosuket@kuhp.kyoto-u.ac.jp (R. Takahashi).
[1] Present address: Toyohashi University of Technology, 1-1, Hibarigaoka, Tenpaku-cho, Toyohashi, Aichi 441-8580, Japan.
[2] Present address: Comparative Genomics Laboratory, National Institute of Genetics, Yata 1111, Mishima, Shizuoka 411-8540, Japan.

0168-0102/$ – see front matter © 2009 Elsevier Ireland Ltd and the Japan Neuroscience Society. All rights reserved.
doi:10.1016/j.neures.2009.10.010

zebrafish, depletion of PINK1 during development causes severe developmental disorders and neurodegeneration (Anichtchik et al., 2008). None of these animal models for PARK6 faithfully recapitulate the pathology of human PD.

In this study, we generated *PINK1* mutant medaka fish by screening our TILLING library (Taniguchi et al., 2006). The *PINK1* mutant medaka showed normal phenotypes for germ-cell lineage, skeletal muscle, and mitochondrial morphology. However, they showed a significant decrease in spontaneous movement during the late stages of life as well as deregulation of dopamine metabolism. The *PINK1* mutant medaka therefore provides a unique opportunity to analyze the causal relationship between dopamine metabolism and neurological symptoms.

2. Materials and methods

2.1. Cloning of medaka PINK1 gene

RNA was extracted from *wild-type* medaka embryos by Trizol (Invitrogen) according to the manufacturer's instructions. cDNA was synthesized using SuperScript III (Invitrogen). To identify medaka *PINK1* orthologs, we used the basic local alignment search tool (BLAST) to search the medaka genome database (http://dolphin.lab.nig.ac.jp/medaka/). Medaka *PINK1* cDNA sequences were then determined using a combination of RT-PCR and rapid amplification of cDNA ends (RACE). RACE products were generated using Seegene's Capfishing kit (Seegene). The 5′ RACE (CCATAGGCCAAGGGCTTGAGCGGGC) and 3′ RACE primers (CCAGTGCCCCCGCTGATGTGCAGTTAGT) were used. The cDNA sequence was used to retrieve the genomic sequence from the draft medaka genome assembly.

2.2. Generation of PINK1 mutant medaka

Generation of *PINK1* mutant medaka was carried out as described previously (Taniguchi et al., 2006). To find the mutations in the region of interest, the genome sequence was amplified with forward primer #1 (TCGGCTTCTACAAGGCTGTT) and reverse primer #1 (CACCCAACTGTGGCTAGTGA) by PCR (92 °C for 60 s; 12 cycles of 92 °C for 20 s, 65 °C for 20 s with a decrement of 0.6 °C per cycle, 72 °C for 30 s; 20 cycles of 92 °C for 20 s, 58 °C for 20 s and 72 °C for 30 s; 72 °C for 180 s [T1 Thermocycler, Biometra]). Sequences were analyzed for the presence of heterozygous mutations using the reverse primer #1. *In vitro* fertilization was carried out using sperm with the desired mutation and the progeny were genotyped by sequencing. Heterozygous fish carrying the same mutation were back-crossed with *Kyoto-Cab*, a substrain of *Cab*, at least 4 times. Furthermore, all the experiments were reproduced using fish back-crossed 7 times or more. Heterozygous fish with this mutation were incrossed to obtain homozygous fish. To verify the genotype of the progeny from this incross, the genome was amplified with forward primer #2 (CAGATTGGGAAAGGATCCAA) and reverse primer #2 (CCCAAAGTTCCACAGCATCT). PCR was carried out according to the following thermocycling program: 94 °C for 120 s; 35 cycles of 94 °C for 30 s, 62 °C for 30 s, 72 °C for 30 s; and 72 °C for 120 s (GeneAmp PCR system9700, Applied Biosystems). 1 μl of PCR product was used as a template for sequencing using BigDYE (Applied Biosystems). Sequencing products were purified by magnetic beads and analyzed using the ABI 3700 DNA Sequencer (Applied Biosystems), following the standard protocol.

2.3. Semi-quantitative RT-PCR

RNA was extracted from the brain for each genotype with Trizol (Invitrogen). cDNA was synthesized using 1 μg RNA for each genotype with SuperScript III (Invitrogen). mRNA expression levels were determined by PCR. For *PINK1*, PCR was carried out using the following thermocycling program: 94 °C for 120 s; 28 cycles at 94 °C for 30 s, 68 °C for 30 s, 72 °C for 30 s; and 72 °C for 120 s (T1 Thermocycler, Biometra). For *β-actin*, the thermocycling program was 94 °C for 120 s; 20 cycles at 94 °C for 30 s, 61 °C for 30 s, 72 °C for 30 s; and 72 °C for 120 s (T1 Thermocycler, Biometra). Forward primer #3 (GAACAGAGCCGTCTTTCTGG) and reverse primer #3 (CCCAAAGTTCCACAGCATCT) were used for *PINK1*. The forward primer (ACTACCTCATGAAGATCCTG) and the reverse primer (TTGCTGATCCACATCTGCTG) were used for *β-actin*.

2.4. In situ hybridization

The digoxigenin (DIG) labeled riboprobe was generated with the DIG RNA labeling kit according to the manufacturer's instructions (Roche). Medaka brains were fixed in freshly prepared 4% paraformaldehyde in PBST. Brains were dehydrated sequentially in methanol. After rehydration, the specimens were treated with 10 μg/ml proteinase K, and treated again in the same fixative for 25 min. The specimens were pre-hybridized in hybridization buffer (HB, 50% formamide, 5× SSC, 5 mg/ml yeast tRNA, 100 μg/ml heparin, 0.1% Tween-20) at 65 °C for 2 h, and then brains were hybridized overnight with the riboprobe in hybridization buffer at 65 °C. Subsequently, brains were washed in decreasing concentrations of SSCT. For probe detection, the embryos were incubated in 0.2% blocking solution (Roche) for 2 h and then rocked overnight with anti-DIG antibody conjugated with alkaline phosphatase (1:7000 dilution, Roche) in 0.2% blocking solution at 4 °C. After several washes with PBST, hybridized probe was detected via color reaction with 450 μg/ml NBT and 175 μg/ml BCIP (Roche). The color reaction was stopped by PBST. Samples were fixed in 4% paraformaldehyde in PBST for 20 min, then embedded in paraffin. Specimens were sliced into 7 μm sections.

2.5. High performance liquid chromatography

Medaka brains were homogenized in 100 μl of 0.4 M $HClO_4$ containing 4 mM $Na_2S_2O_5$ and 4 mM diethylenetriaminepentaacetic acid. Supernatant by centrifugation at 18,500 × *g* for 5 min was used to measure free catechols. High performance liquid chromatography (HPLC) was conducted with a mobile phase containing buffer A:acetonitrile:methanol (1000:25.9:62.9, v/v) (buffer A: 0.1 M phosphate, 0.05 M citrate, 4 mM sodium 1-heptanesulfonate and 0.1 mM EDTA, pH 3.0). Catecholamine and its metabolites were identified using a series coulometric detector (ESA, Inc.). Data were collected and processed using CHROMELEON™ Chromatography Data Systems 6.40 (Dionex). The pellet was reserved for analysis of the protein content. For this purpose, the pellet was solubilized in 100 μl of 0.5N NaOH at 60 °C and the protein was quantified by means of a BCA assay (Pierce) using bovine serum albumin (BSA) as the standard.

2.6. Hematoxylin–eosin staining

Entire medaka bodies or individual organs were fixed in 4% paraformaldehyde for 24 h, embedded in paraffin, then sliced into 10-μm sections. Hematoxylin–eosin (HE) staining was done using standard protocols.

2.7. Transmission electron microscope and Toluidine blue staining

To prepare for electron microscopy, male testes and muscle tissue were fixed overnight in 2% gluteraldehyde with a 0.1 M cacodylate buffer. After rinsing in a 0.1 M cacodylate buffer with 0.1 M sucrose, samples were postfixed in 1% OsO_4, with a 0.1 M

cacodylate buffer and 0.1 M sucrose for 1.5 h. Samples were rinsed, dehydrated in an ethanol series, and embedded in Epon. The 1-μm sections were stained with Toluidine blue, and the 50–80 nm sections were stained with uranyl acetate and lead citrate.

2.8. Immunohistochemistry

Medaka brains were fixed in 4% paraformaldehyde for 24 h and embedded in paraffin. Each brain was sliced into 20 μm sections to prepare for TH immunohistochemistry. Immunohistochemical analysis (1:500, mouse anti-TH, MAB318, Millipore) was carried out on every section using the Vector Elite ABC kit with DAB. The number of dopaminergic neurons in the middle diencephalon was determined by counting the TH-immunopositive (TH^+) neurons in the coronal sections using an OLYMPUS BX51 microscope with a MICROFIRE digital camera (Olympus) and Stereo Investigator (MBF Bioscience).

2.9. TdT-mediated dUTP nick-end labeling assay

Brains were fixed in 4% paraformaldehyde for 24 h and embedded in paraffin. Each brain was sliced into 5 μm sections in preparation for a TUNEL assay. Apoptotic cells were detected by the TUNEL method using an *in situ* Apoptosis Detection Kit (TaKaRa Bio Inc.), according to the manufacturer's protocol.

2.10. Western blot analysis

Brains were homogenated in a RIPA buffer (25 mM Tris–HCl [pH 7.6], 150 mM NaCl, 1% NP-40, 1% sodium deoxycholate, 0.1% SDS) with protease inhibitors and processed for SDS-PAGE analysis. Immunoreactive bands were detected with ECL reagent or ECL plus reagent (GE Healthcare Life Sciences) and the chemiluminescent signal was visualized by exposing the membrane to Fuji RX X-ray film (Fuji Film). The film was scanned and densitometric analysis of blots was performed using ImageJ software (National Institute of Health). The background intensity of the film was subtracted from the band intensity. Anti-medaka parkin polyclonal antibody was raised against full-length medaka parkin protein and used for the analysis (1:500). Anti-TH monoclonal antibody (1:1000, mouse anti-TH, MAB318, Millipore) was used for the Western blot analysis of the TH. Anti-β-actin monoclonal antibody (1:5000, AC-15, Sigma–Aldrich) was used for the loading control. Parkin-deficient medaka, used for a negative control, was generated as described previously (Taniguchi et al., 2006).

2.11. Behavioral analysis

The medaka were tested for spontaneous swimming. Images were collected using a video camera positioned above the tank under low intensity, indirect white light, then analyzed by a computer-assisted system (Muromachi Kikai). The water tank was a transparent circular container (20 cm diameter, 2 cm water depth, 27 °C). Upon introduction into the tank, all adult fish remained motionless for several minutes, then began to swim. Filming began 1 min after the medaka began to swim and lasted for 5 min. We defined *movement* as occurring when a medaka moved more than 0.1 cm per 0.1 s. Total swimming distance (cm), duration of swimming movement (s) and swimming velocity (total swimming distance/duration of swimming movement) were measured and compared across groups.

2.12. Statistical analysis

Data were expressed as mean ± standard error of the mean (SEM). Results were statistically evaluated for significance using the ANOVA test with post hoc analysis using Dunnet's test or logrank test for survival analysis. Differences were considered significant when $p < 0.05$.

3. Results

3.1. Cloning of medaka PINK1

Only a single ortholog of the human *PINK1* gene was identified (by BLAST search) in the draft medaka genome. The medaka *PINK1* gene has 8 exons and encodes a protein consisting of 577 amino acids (Fig. 1A and B). The medaka PINK1 amino acid sequence has 54.1% homology to human PINK1. The kinase domain was highly conserved between the two species (Fig. 1B).

3.2. Generation of PINK1 mutant medaka

To generate *PINK1* mutant medaka, we targeted exons 2 and 3 of the *PINK1* gene for nucleotide sequencing. We sequenced the genomes of 5771 samples obtained from ENU-mutagenized medaka. We identified 14 mutations in total, 6 of which were silent mutations (Table 1). From the eight other mutations, we selected a nonsense mutation, Q178X, for further study because it resulted in the disruption of the kinase domain. It has been reported that human PARK6 patients carry similar truncation mutations (Q239X, R246X, Y258X, W437X, Q456X, R492X) in the kinase domain (Valente et al., 2004; Hedrich et al., 2006; Hatano et al., 2004; Tan et al., 2006).

From the incross of heterozygous Q178X mutant parents, we obtained the expected numbers (according to Mendelian inheritance [Fig. 3A]) of *wild-type* fish ($PINK1^{WT/WT}$), heterozygous mutants ($PINK1^{WT/Q178X}$), and homozygous mutants ($PINK1^{Q178X/Q178X}$) (Fig. 2A). Semi-quantitative RT-PCR showed a marked reduction of *PINK1* mRNA in the $PINK1^{Q178X/Q178X}$ medaka, probably due to the nonsense-mediated mRNA decay (Fig. 2B). We therefore concluded that we had succeeded in generating PINK1-deficient medaka fish.

3.3. Distribution of medaka PINK1 mRNA

To characterize medaka *PINK1* expression, we visualized medaka *PINK1* mRNA by *in situ* hybridization. The anti-sense RNA probe exhibited diffuse signals in the gray matter of $PINK1^{WT/WT}$ medaka brain (Fig. 4A–E). The telencephalon and diencephalon that contain striatum and many dopaminergic neurons respectively showed moderate anti-sense signals (Fig. 4A–C). The optic tectum disclosed relatively intense signals comparing to other regions (Fig. 4B and C). On the other hand, the signals of hindbrain and spinal cord were weak (Fig. 4D and E). We further investigated medaka *PINK1* mRNA expression in $PINK1^{Q178X/Q178X}$ medaka. In this case, we could not detect the signals of anti-sense probe (Fig. 4F–J). This finding suggested the signals of anti-sense probe was specific to medaka *PINK1* mRNA and again supported the degradation of *PINK1* mRNA in $PINK1^{Q178X/Q178X}$ medaka.

3.4. $PINK1^{Q178X/Q178X}$ medaka showed normal development and mild shortening of life span

Like human PARK6 patients, $PINK1^{Q178X/Q178X}$ medaka grew normally for 12 months without any obvious morphological abnormalities or developmental disorders. Remarkably, the $PINK1^{Q178X/Q178X}$ medaka showed a significant decrease in life span, when compared with $PINK1^{WT/WT}$ and $PINK1^{WT/Q178X}$ fish (the $PINK1^{Q178X/Q178X}$ medaka began to die at 12 months) (Fig. 3B). This diminished life expectancy was not caused by increased tumorigenesis (data not shown).

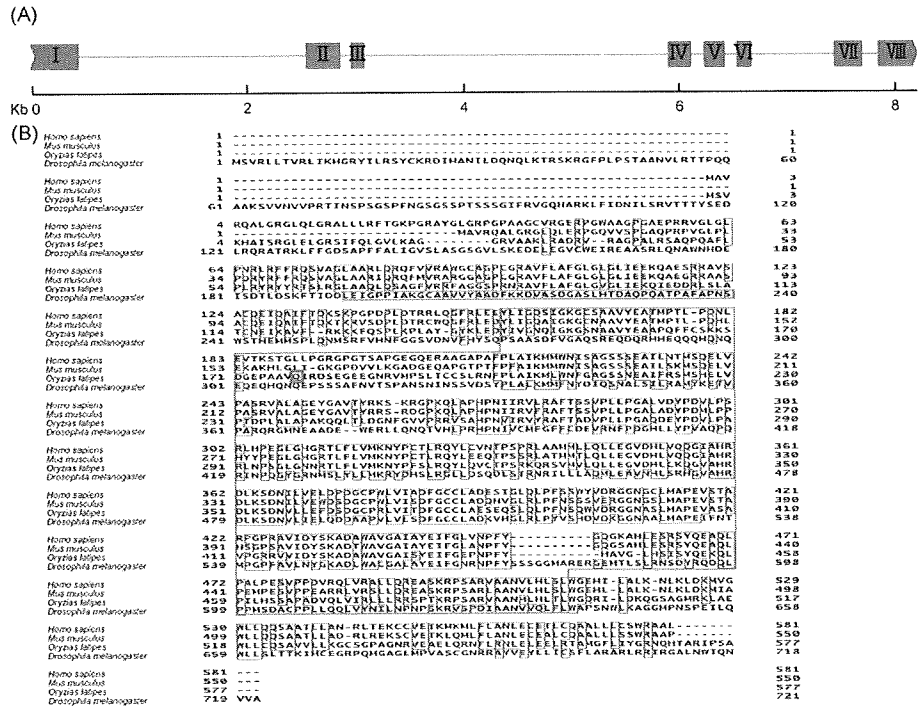

Fig. 1. Medaka PINK1 profiles. (A) Genome structure of medaka *PINK1* gene. The red boxes indicate each exon (with the Greek numeral representing the number of the exon) and the bar represents the intron. (B) Sequence alignment of human, mouse, medaka and *Drosophila melanogaster* PINK1 protein. Amino acids conserved among three or four species are outlined in red. The medaka PINK1 amino acid sequence has 54.1% homology to human PINK1. The kinase domain, which is highly conserved across the two species, is outlined in light blue. The green outlining signifies the Q178X mutation in the mutant medaka. (For interpretation of the references to color in this figure legend, the reader is referred to the web version of the article.)

3.5. *PINK1*$^{Q178X/Q178X}$ medaka show reduced body weight at the late-adult stage

To investigate the cause of this shortened life expectancy, we measured the body weight of the *PINK1*$^{Q178X/Q178X}$ medaka over time. We placed ten 8-month-old fish from each genotype into separate tanks for 4 months. There was no significant difference in body weight among medaka with the *PINK1*$^{WT/WT}$, *PINK1*$^{WT/Q178X}$, and *PINK1*$^{Q178X/Q178X}$ genotypes during this time (Fig. 5A). Nor were there significant differences in body weight when medaka representing all three genotypes were maintained together in one tank for 8 months. However, at 12 and 18 months, the body weight of the *PINK1*$^{Q178X/Q178X}$ medaka increased at a slower rate, compared with the *PINK1*$^{WT/Q178X}$ and *PINK1*$^{Q178X/Q178X}$ medaka when all the genotypes were maintained together (Fig. 5B). These findings imply that older *PINK1*$^{Q178X/Q178X}$ medaka were not able to compete for limited amounts of food with littermates carrying the other genotypes.

Table 1
List of *PINK1* mutations from our TILLING library showing mutated nucleotides and resulting changes of the transcript.

DNA sequence	Amino acid substitution	Result
AGGACACTTC (A>G) TTTACATACC		Intron
TGCAGGCGGT (G>A) TTCAGAAAGA	V121V	Silent
AAAGAAGAAG (T>C) TCCAGAGCCC	F127L	Substitution
AACTGGAGGA (T>C) TACATTGTAG	D142D	Silent
AAAGGATCCA (A>G) CGCAGCTGTG	N154S	Substitution
GCTGTGTATG (A>G) AGCTGCACCT	E159G	Substitution
CCAAGAAAAG (C>T) GATGGTGAGC	S170S	Silent
CGCCGCGGTG (C>T) AGATACGAGA	Q178X	Truncation
GCTGTGGAAC (T>C) TTGGGGTGGG	F212L	Substitution
TGTGATTCTA (T>A) GTGTTTGCAG		Intron
TTCCCACAGA (C>T) CCCCTCGCTC	D233D	Silent
CGCTCTGGCG (C>A) CAGCAAAACA	P239T	Substitution
GCTCTGGCGC (C>T) AGCAAAACAG	P239L	Substitution
CGCCAGCAAA (A>G) CAGCAACTTA	K241K	Silent

(A>B): A is the nucleotide of *wild-type* Kyoto-cab and B is the nucleotide of the mutant. Of the 14 types of mutation in the genome, 2 were located in the intron, 5 resulted in silent change of the amino acid sequence, 6 were amino acid substitutions and 1 was a truncation of the transcript. The mutation we selected (Q178X) is underlined.

3.6. Muscle, sperm, and mitochondria intact in *PINK1*$^{Q178X/Q178X}$ medaka

PINK1-deficient *Drosophila* show male sterility, skeletal muscle and sperm degeneration, and abnormal mitochondria morphology. We therefore inspected the morphology of these tissues in medaka. Contrary to the *Drosophila* model, the skeletal muscle and sperm appeared to be normal in the *PINK1*$^{Q178X/Q178X}$ medaka (Fig. 6A–D). Nor did the mitochondria in the skeletal muscle (Fig. 6E and F) or sperm show any abnormal morphology (data not shown). Both male and female *PINK1*$^{Q178X/Q178X}$ medaka were consistently fertile (data not shown). Thus, deletion of PINK1 causes a significantly less abnormal phenotype of muscle and sperm in medaka than in *Drosophila*.

3.7. Amount of parkin indistinguishable across genotypes

Familial PD (PARK2) is caused by mutations of the gene-encoding E3 ubiquitin ligase, *parkin* (Kitada et al., 1998). Since studies of the *PINK1*-silenced zebrafish and *D. melanogaster* found a reduction of *parkin* mRNA and parkin protein, respectively (Anichtchik et al., 2008; Yang et al., 2006), we used Western blot analysis to measure parkin protein. The amount of parkin was comparable in the *PINK1*$^{WT/WT}$, *PINK1*$^{WT/Q178X}$, and *PINK1*$^{Q178X/Q178X}$ medaka (Fig. 7).

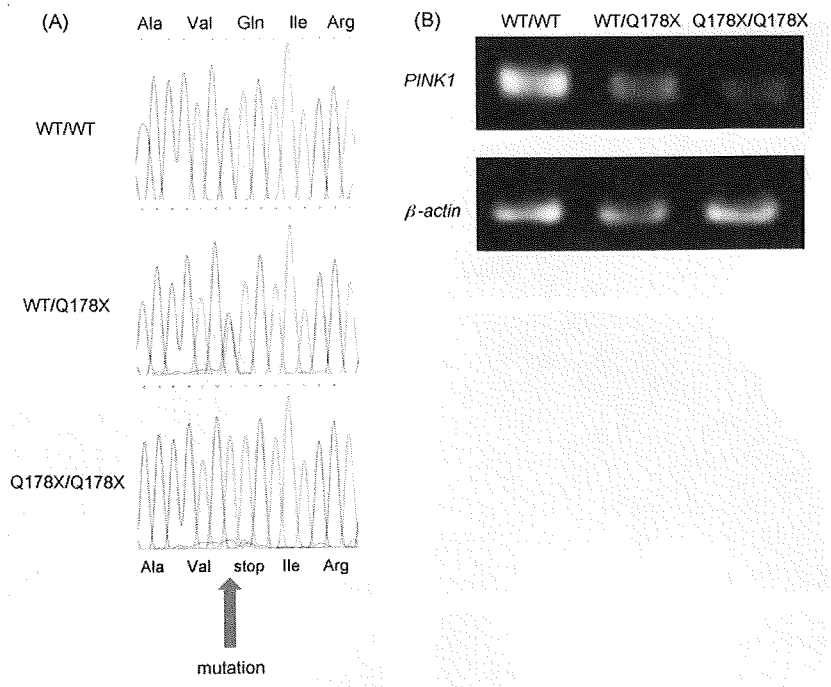

Fig. 2. Generation of *PINK1*$^{Q178X/Q178X}$ medakas. (A) Sequence data for each genotype. A = green, T = red, G = black, and C = blue. The three-letter amino acid codes show the resulting transcript. The top figure illustrates the *PINK1*$^{WT/WT}$ medaka sequence, while the middle and bottom figures illustrate heterozygous and homozygous Q178X mutation in *PINK1*$^{WT/Q178X}$ and *PINK1*$^{Q178X/Q178X}$ medaka, respectively. The C to T mutation of the genome results in a TAG stop codon (red arrow). (B) Semi-quantitative RT-PCR of *PINK1* mRNA for each genotype. The upper and lower lanes show the RT-PCR results of *PINK1* and *β-actin* (control) mRNA, respectively. The *PINK1* mRNA of the *PINK1*$^{Q178X/Q178X}$ medaka decreased markedly compared with *PINK1*$^{WT/WT}$ and *PINK1*$^{WT/Q178X}$. This reduction may be due to nonsense-mediated mRNA decay. (For interpretation of the references to color in this figure legend, the reader is referred to the web version of the article.)

3.8. No significant dopaminergic cell loss in *PINK1*$^{Q178X/Q178X}$ medaka

Dopaminergic cell loss and the denervation of the striatum constitute the representative pathology of human PD patients. Having previously identified tyrosine-hydroxylase-positive (TH^+) dopaminergic neurons and noradrenergic neurons in the medaka brain, as well as selective loss of TH^+ dopaminergic neurons in MPTP-treated medaka (Matsui et al., 2009), we histologically examined the TH^+ neurons. The number of cells in the middle diencephalon did not decrease in the *PINK1*$^{Q178X/Q178X}$ medaka, when compared with medaka carrying the other genotypes, even at 18 months (Fig. 8A–E). Western blot analysis of the whole brain indicated a similar amount of TH protein in each genotype (Fig. 8I). The *PINK1*$^{Q178X/Q178X}$ medaka did not display pathological abnormalities in dopaminergic neurons in other regions or in noradrenergic neurons in the medulla oblongata (data not shown). We continued to inspect TH immunohistochemistry, focusing on the striatum, because we previously found that the striatum contains the terminals of dopaminergic neurons, and also because denervation of the striatum is observed in human PD patients. The distribution of dopaminergic neurons in the striatum showed no detectable abnormalities in the *PINK1*$^{Q178X/Q178X}$ medaka (Fig. 8G and H). To analyze apoptotic cells, we performed a TUNEL assay on the whole brain. Virtually no apoptotic cell death was present in either the *PINK1*$^{Q178X/Q178X}$ or the control medaka (data not shown). In sum, the *PINK1*$^{Q178X/Q178X}$ medaka showed no prominent defect in the number or morphology of dopaminergic and noradrenergic neurons.

(A)

Genotype	1dpf	3month
WT/WT	12 (24.0%)	22 (26.8%)
WT/Q178X	25 (50.0%)	40 (48.8%)
Q178X/Q178X	13 (26.0%)	20 (24.4%)
total	50	82

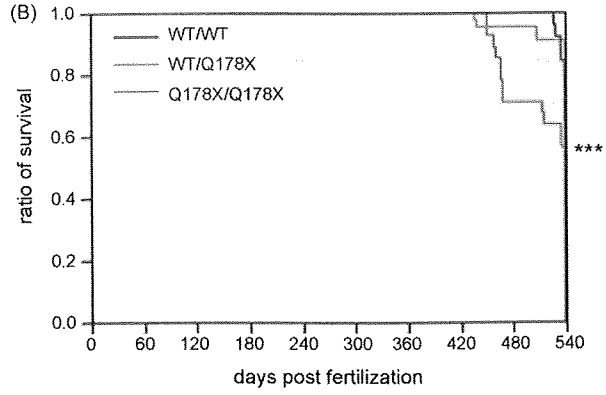

Fig. 3. Mendelian inheritance of Q178X mutation and survival curves of *PINK1*$^{Q178X/Q178X}$ medaka. (A) The ratio of genotypes in newborn and 3-month-old medaka with *PINK1*$^{WT/Q178X}$ parents. Both results agree with Mendelian inheritance. These Mendelian ratios suggest no difference in mortality rates in the developmental/larval stage. (B) Survival curve for each genotype. End point is the death of each medaka or day 540. The results show mild but significant shortening of the life span in *PINK1*$^{Q178X/Q178X}$ medaka ($n = 28$), comparing with *PINK1*$^{WT/WT}$ ($n = 26$) or *PINK1*$^{WT/Q178X}$ ($n = 46$). ***$p < 0.001$ vs. *PINK1*$^{WT/WT}$.

3.9. Abnormal amount of dopamine and DOPAC in the absence of *PINK1* in the brains of young and old fish

A decreased amount of catecholamine is the most prominent feature of human PD patients. We therefore measured the amount of dopamine and norepinephrine in the whole brain of *PINK1*$^{Q178X/Q178X}$ medaka at 4, 8, 12 and 18 months. The amount of norepinephrine did not differ across genotypes (Fig. 9C). Unlike with human PD patients, the amount of dopamine in the medaka carrying *PINK1*$^{Q178X/Q178X}$ as well as the other genotypes was very similar at 12 and 18 months. However, to our surprise, the amount

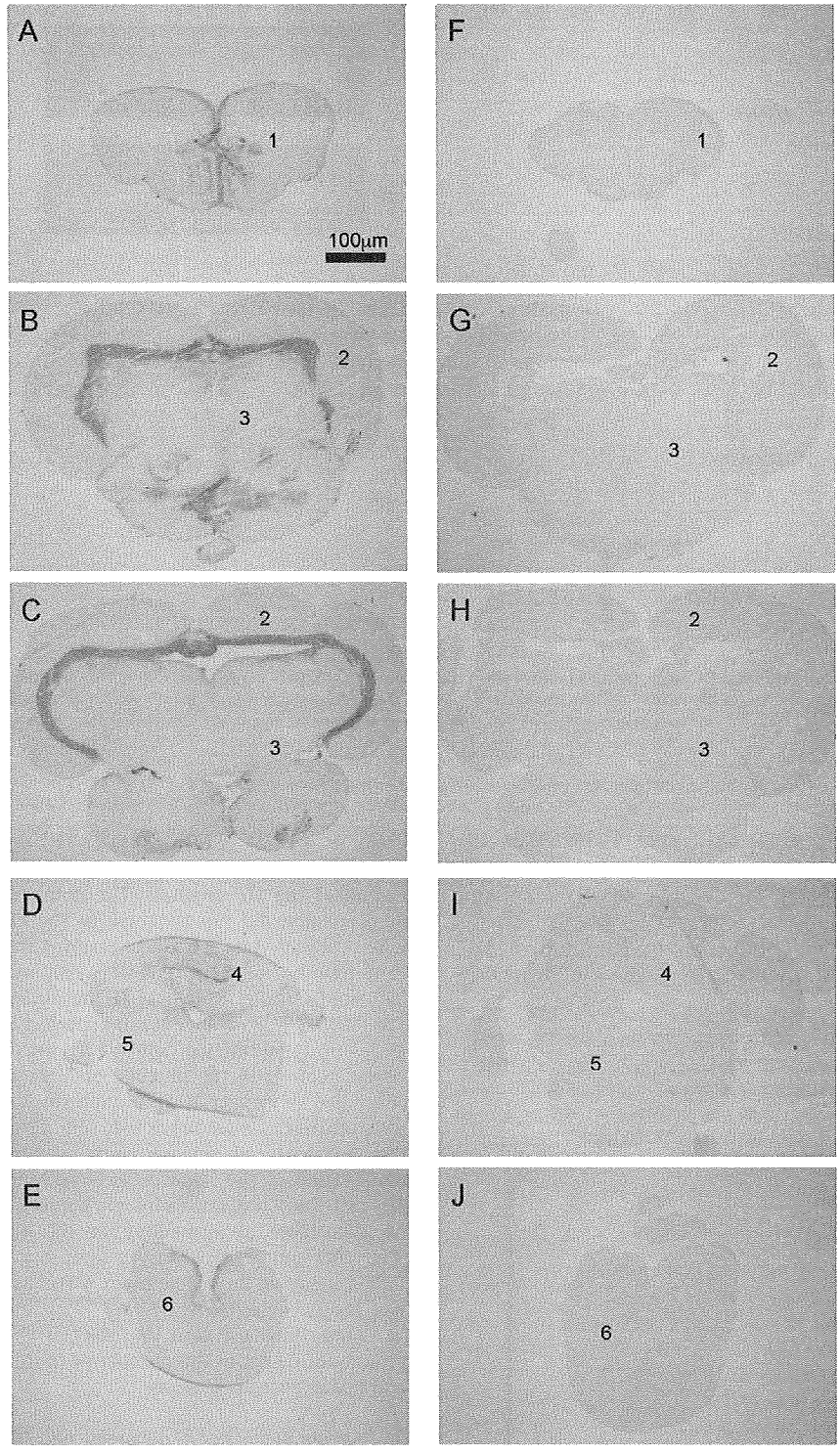

Fig. 4. *In situ* hybridization of medaka *PINK1* mRNA. Anti-sense signals of *PINK1*$^{WT/WT}$ medaka brain (A–E) and *PINK1*$^{Q178X/Q178X}$ medaka brain (F–J) (12 months). (1) Telencephalon, (2) optic tectum, (3) diencephalon, (4) cerebellum, (5) medulla oblongata and (6) spinal cord.

of dopamine in the *PINK1*$^{Q178X/Q178X}$ medaka brain was higher than that of the *PINK1*$^{WT/WT}$ at both 4 and 8 months (Fig. 9A). By 12 months, the levels of dopamine were the same for all genotypes, and they remained the same at 18 months (Fig. 9A). If the elevated dopamine were functional, these fish might be expected to move more frequently than fish carrying the other genotypes. In fact, the *PINK1*$^{Q178X/Q178X}$ medaka moved less frequently than did the fish carrying the other genotypes (Fig. 10A–C), suggesting that the elevated dopamine levels reflect deregulation of dopamine metabolism, including the defective release of dopamine from the neurons. This idea is supported by the fact that the amount of 3,4-dihydroxyphenylacetic acid (DOPAC), a metabolite of dopa-

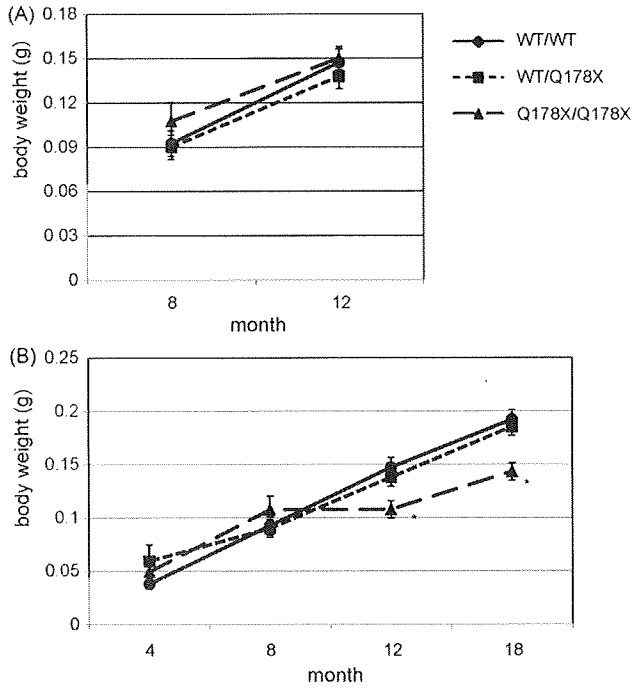

Fig. 5. Body weight of *PINK1*$^{Q178X/Q178X}$ medaka. (A) Body-weight curves for fish separated by genotype at 8 months. No significant differences were seen (n = 10 for each group). (B) Body-weight curves for fish not separated by genotype. A reduced increase in body weight was observed for the *PINK1*$^{Q178X/Q178X}$ medaka at 12 and 18 months (n = 15 for each group). $^{*}p < 0.05$ vs. *PINK1*$^{WT/WT}$.

mine, decreased. We conclude that the loss of PINK1 causes dysregulation of dopamine metabolism without affecting the survival of dopaminergic neurons.

3.10. *PINK1*$^{Q178X/Q178X}$ mutation causes reduction of spontaneous swimming only at 12 and 18 months

Late-onset reduction of spontaneous movement is one of the key symptoms found in human PD patients. We therefore quantified spontaneous swimming movement in *PINK1*$^{Q178X/Q178X}$ medaka. All fish showed comparable movement at 4 and 8 months, irrespective of the genotype of the *PINK1* gene. Remarkably, the *PINK1*$^{Q178X/Q178X}$ medaka displayed a significant reduction of spontaneous swimming at 12 and 18 months, in comparison with fish carrying the other genotypes (Fig. 10A–D). These significant decreases were confirmed by all examined swimming parameters: total distance, duration of movement, and velocity. We therefore conclude that the loss of PINK1 causes late-onset reduction of spontaneous swimming movement.

4. Discussion

Japanese medaka (*Oryzias latipes*) is easy to handle and produce large numbers of progeny per generation. It has several advantages over zebrafish in modeling PD. First, the whole genome has been sequenced and assembled since the size of medaka genome is only 700 Mb, half the size of the zebrafish genome. Second, several inbred strains have been established in medaka, but not in zebrafish. The lack of genetic variations among individuals may simplify and facilitate genetic studies, and is particularly important for disease models. Third, cryopreservation of the sperm is easy and reliable, so we can maintain and store numerous strains in the laboratory. Considering the merits that are above-mentioned, we can regard medaka as one of the attractive vertebrate (*Drosophila* is not vertebrate) animal models.

In this report, we verified that the *PINK1*$^{Q178X/Q178X}$ medaka is a novel animal model suitable for use to investigate the pathogenesis of PD. Mutant fish display a phenotype very close to that of human PD patients. This phenotype includes normal development and growth, mild shortening of the life span, late-onset reduction of spontaneous movement, and a decrease in the amount of dopamine metabolic product (DOPAC). The establishment of the medaka PD model will allow for extensive genetic analysis in the future, using multiple gene disruption and expression of transgenes with large numbers of fish.

By analyzing the medaka PD model over time, we were able to determine the level of dopamine and its metabolic products in the brain. We found that the loss of PINK1 function affects the metabolism of dopamine in the central nervous system. Indeed, the amount of DOPAC decreased between the 4 and 18 months. Unexpectedly, we observed a higher, rather than a lower, amount of dopamine in the brains of 4- and 8-month-old *PINK1*$^{Q178X/Q178X}$ medaka compared to *PINK1*$^{WT/WT}$. This appears to be similar to the results of a study using *PINK1*-shRNA-expressing transgenic mice, which showed increased amounts of dopamine (Zhou et al., 2007). In another study, gene disruption of *PINK1* was found to impair the release of dopamine from neurons in the striatum, though the dopamine levels were not documented (Kitada et al., 2007). In our study, the increased level of dopamine was not associated with an increase in spontaneous movement in young *PINK1*$^{Q178X/Q178X}$ medaka. Taking these observations together, it seems that one possible scenario is that the *PINK1*$^{Q178X/Q178X}$ medaka are incapable of effectively releasing dopamine as a neuronal transmitter, leading to the accumulation of dopamine in the neuronal cells. This accumulated dopamine might harm the neurons, because the metabolism of dopamine is accompanied by the generation of oxidative radical species (Blum et al., 2001). Whether or not the amount of dopamine also increases in the brain of human PARK6 patients prior to the appearance of PD-related symptoms should be investigated.

The late-adult-onset phenotype of the *PINK1*$^{Q178X/Q178X}$ medaka is in marked contrast with the more prominent phenotypes of PINK1-depleted zebrafish and *D. melanogaster*. In zebrafish, the Morpholino-mediated suppression of PINK1 caused developmental disorders as well as neurodegeneration (Anichtchik et al., 2008). This severe phenotype of PINK1-depleted zebrafish is surprising. The different phenotypes of the two models might be attributable to the difference of species or strategies. Morpholino may have off-target effect (Ekker and Larson, 2001). On the other hand, non-negligible mutations by ENU may remain although backcross progeny have been analyzed. In *D. melanogaster*, the loss of PINK1 resulted in selective defects in dopaminergic neurons, skeletal muscle, sperm, and mitochondria. It should be noted that the phenotype associated with the loss of PINK1 is distinctly different in model animals such as medaka, zebrafish, mouse, and *D. melanogaster*. The genetic study of *Drosophila* provides compelling evidence that PINK1 works in the same pathway as does parkin. In fact, the loss of function in parkin, *PINK1*, or both genes will result in the same pathology in *Drosophila* (Clark et al., 2006; Park et al., 2006; Yang et al., 2006). An important question that needs to be solved in near future is whether the genetic relationship demonstrated in *Drosophila* is also observed in other PD model animals, including medaka.

Diffuse signal pattern of medaka *PINK1* mRNA in the gray matter is consistent with that of rat and mouse *PINK1* (Taymans et al., 2006). The distribution of *PINK1* mRNA is not restricted to the dopaminergic neurons in rat, mouse and our medaka fish. This makes it difficult to explain why loss of PINK1 function leads to the dysfunctions of dopaminergic neurons. The ways to prove the

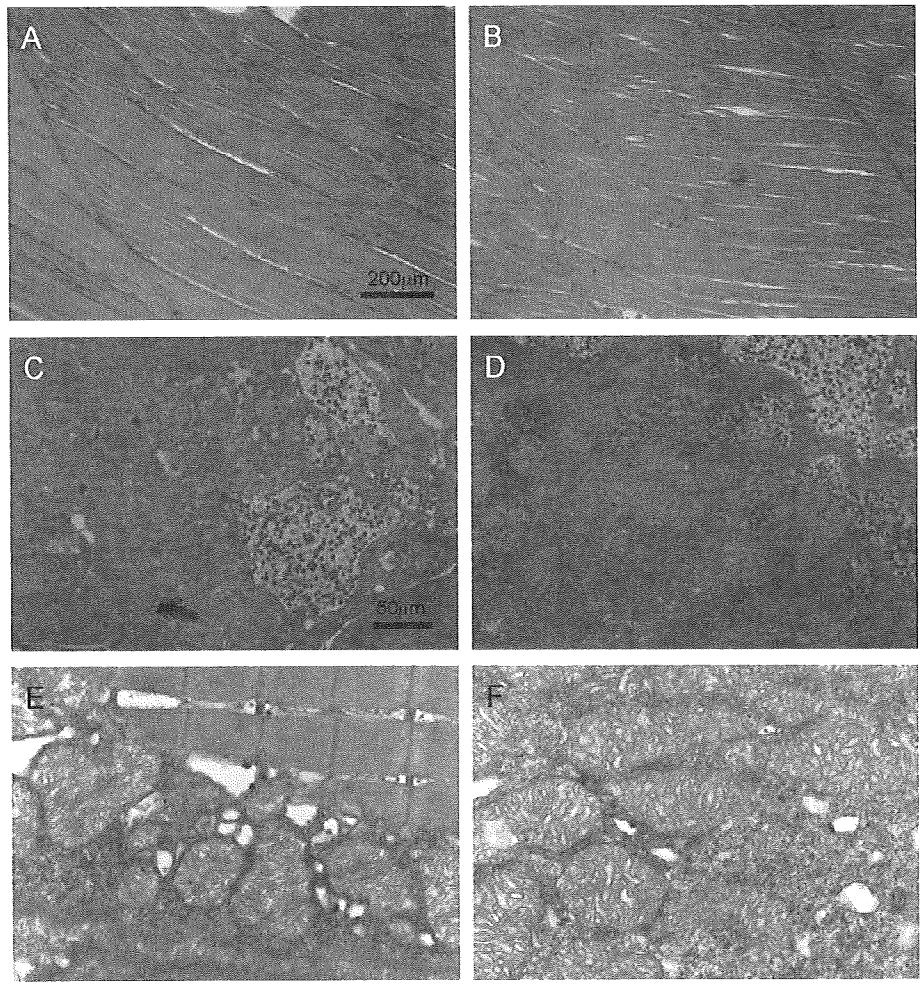

Fig. 6. Histological analysis of muscle and testes in *PINK1*$^{Q178X/Q178X}$ medaka fish (12 months). (A, C, and E) PINK1$^{WT/WT}$. (B, D, and F) *PINK1*$^{Q178X/Q178X}$. (A and B) Hematoxilin–eosin staining of the muscle. (C and D) Toluidine blue staining of the testes. (E and F) Electron-microscopic image of mitochondria in the muscle. (A–F) Muscles, testes and mitochondria are intact in the *PINK1*$^{Q178X/Q178X}$ medaka. (F) Altered cristae morphology, fragmentation or elongation of mitochondria were not detected. (For interpretation of the references to color in this figure legend, the reader is referred to the web version of the article.)

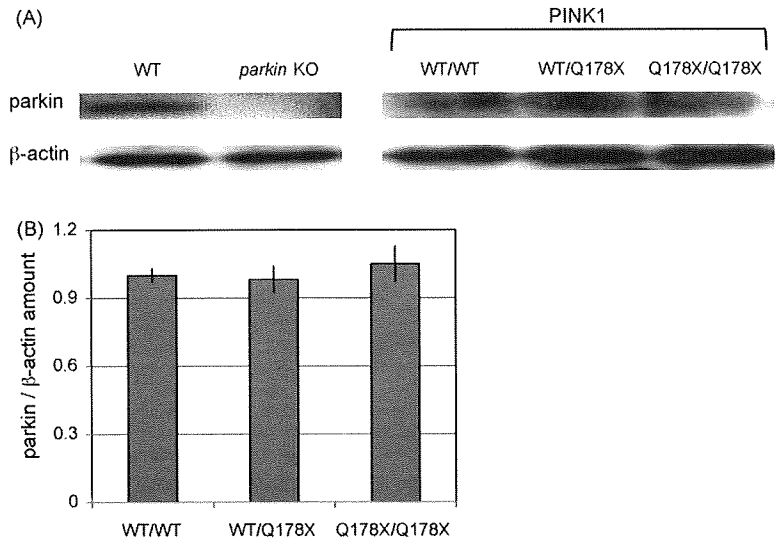

Fig. 7. Amount of parkin protein in *PINK1*$^{Q178X/Q178X}$ medaka (18 months). (A) Amount of protein in medaka parkin examined by Western blot analysis. (B) Ratio of parkin/β-actin (loading control) for each genotype (average amount for *PINK1*$^{WT/WT}$ medaka = 1). The amount of parkin does not differ across genotypes ($n = 6$ for each group).

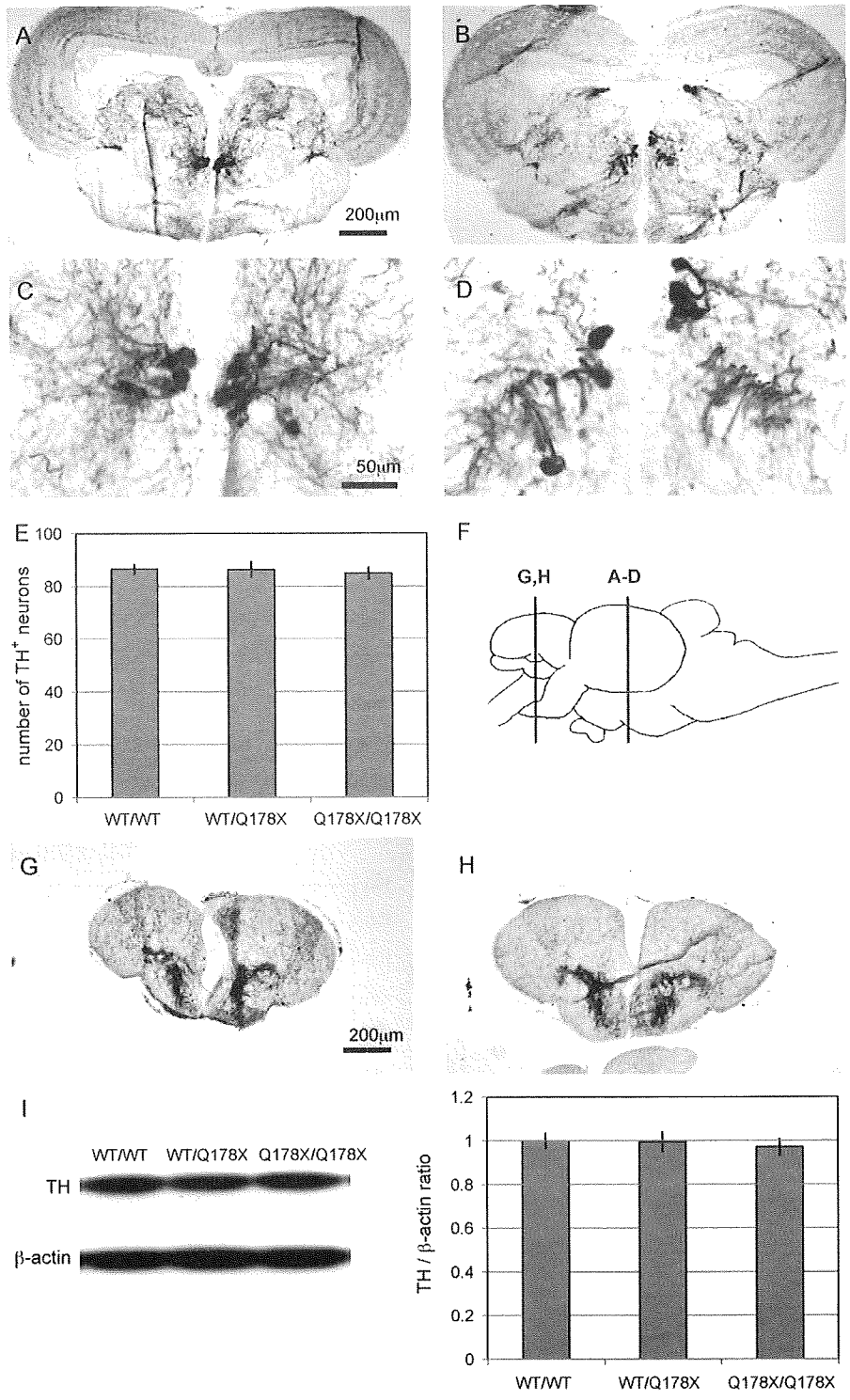

Fig. 8. Immunohistochemistry of tyrosine-hydroxylase and Western blot analysis of *PINK1*$^{Q178X/Q178X}$ medaka. Coronal sections of striatum and middle diencephalon. (A–D) Representative photographs of middle diencephalic dopaminergic neurons in *PINK1*$^{WT/WT}$ (A and C) and *PINK1*$^{Q178X/Q178X}$ (B and D) medaka at 18 months. (E) The number of tyrosine-hydroxylase positive (TH^+) neurons does not differ across genotypes (n = 10 for each group). (G) Striatum dopaminergic fibers for *PINK1*$^{WT/WT}$ and (H) *PINK1*$^{Q178X/Q178X}$ medaka at 18 months. The striatum of the *PINK1*$^{Q178X/Q178X}$ medaka is indistinguishable from that of *PINK1*$^{WT/WT}$. (F) Map of medaka brain; A–F indicate the section levels of A–D, F and G. (I) Amount of TH protein in the whole brain at 18 months, examined by Western blot analysis and normalized by β-actin (loading control). The graph shows the ratio of tyrosine-hydroxylase (TH)/β-actin for each genotype (average amount for *PINK1*$^{WT/WT}$ medaka = 1). The amount of TH does not differ across genotypes (n = 6 for each group).

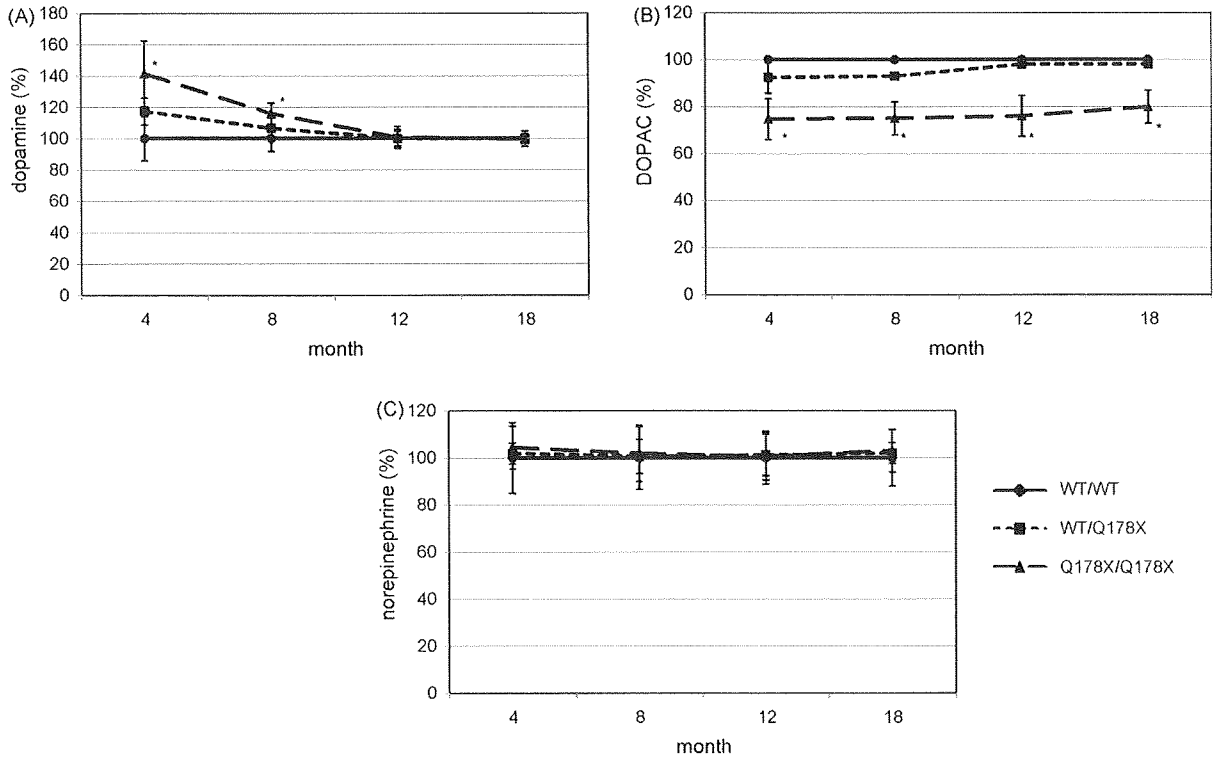

Fig. 9. Amount of dopamine, DOPAC, and norepinephrine in the brain of *PINK1*$^{Q178X/Q178X}$ medaka. All values are expressed as a percentage of the amount (ng) per protein weight (mg) for *PINK1*$^{WT/WT}$ (n = 10 for each group). (A) The amount of dopamine in the *PINK1*$^{Q178X/Q178X}$ medaka brain was higher at 4 and 8 months, then registered as normal at 12 and 18 months. (B) The amount of DOPAC decreased at every stage examined. (C) The amount of norepinephrine in the *PINK1*$^{Q178X/Q178X}$ medaka brain was comparable to that in *PINK1*$^{WT/WT}$. $^{*}p < 0.05$ vs. *PINK1*$^{WT/WT}$.

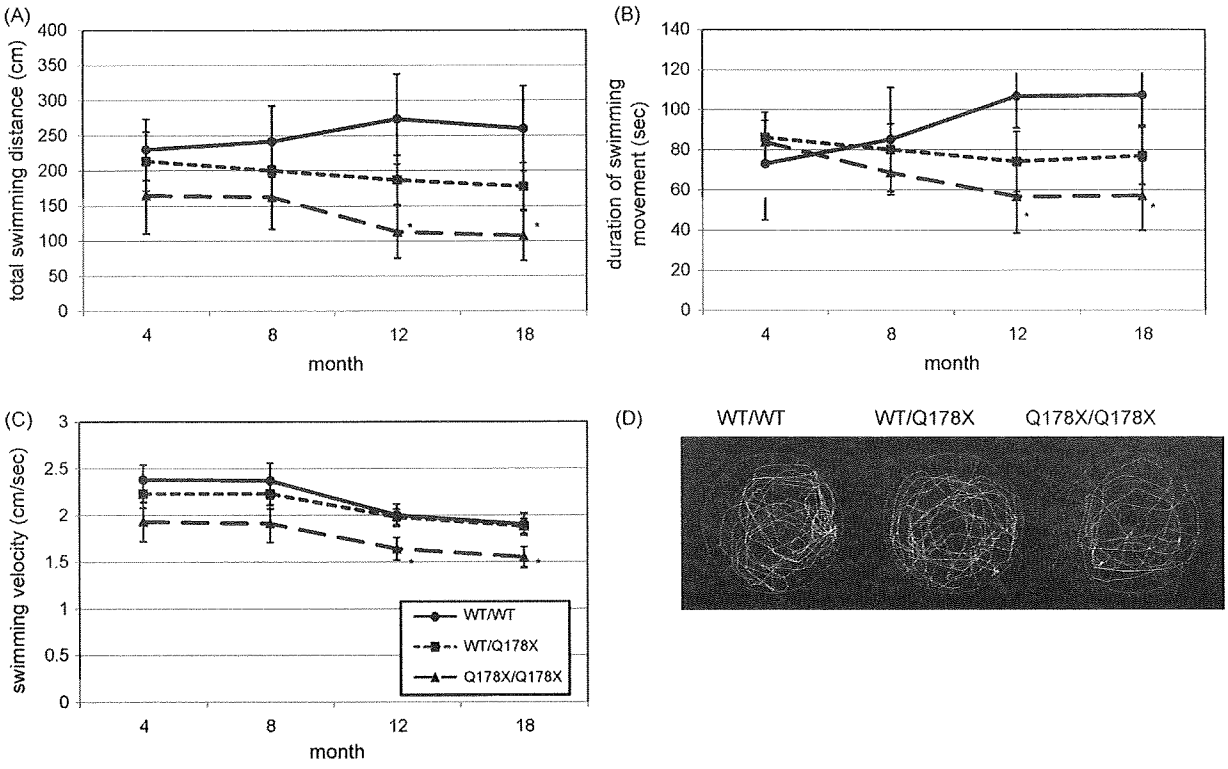

Fig. 10. Spontaneous swimming movement for *PINK1*$^{Q178X/Q178X}$ medaka. (A) Total swimming distance (cm). (B) Duration of swimming movement (s). (C) Swimming velocity (cm/s). (D) Representative tracks for each genotype. Each genotype showed comparable movement at 4 and 8 months. All parameters for the *PINK1*$^{Q178X/Q178X}$ medaka decreased at 12 and 18 months (n = 15 for each group). $^{*}p < 0.05$ vs. *PINK1*$^{WT/WT}$.

genotype–phenotype relationship include complementing the putative causal allele *in vivo* or *in vitro* by transgenesis or retroviral transduction, non-complementation of a null allele generated by homologous recombination, or backcrossing for many generations to the outcross strain (Cook et al., 2006). Therefore, we conducted the overall experiments using not only 4–6 times back-crossed fish but also fish back-crossed more than 7 times. They all showed the same results, suggesting that loss of PINK1 function indeed resulted in the phenotypes shown in this manuscript. However, we analyzed only a single line of *PINK1* mutant and did not perform rescue experiments using transgenic medaka fish in this study. Therefore further experiments are necessary to elucidate the genotype–phenotype relationship.

In conclusion, this report reveals a new *in vivo* function for PINK1. PINK1 affects the metabolism of dopamine in the brain long before the loss of dopaminergic neurons. PINK1-deficient medaka exhibited decreased spontaneous movement only at the late-adult stage, a phenotype that recapitulates a typical symptom of PD. We recently generated another PD model by treating fish with a chemical neurotoxin, MPTP, a standard method used to induce PD (Matsui et al., 2009). The treatment indeed induced the loss of dopaminergic cells and movement disorder. The medaka PD models can therefore contribute significantly to our understanding of the molecular mechanisms underlying the pathology of PD.

Acknowledgements

We are grateful to the members of the Department of Neurology, Kyoto University, and to Dr. Hideaki Takeuchi and Yuji Suehiro of Tokyo University, for their helpful advice. We thank Prof. Takahiko Yokoyama of the Department of Anatomy and Developmental Biology, Kyoto Prefectural University of Medicine for *in situ* hybridization experiment. We also thank the technical staff of the Department of Radiation Genetics, Kyoto University and the Sequence Technology Team at RIKEN GSC for their assistance.

References

Anichtchik, O., Diekmann, H., Fleming, A., Roach, A., Goldsmith, P., Rubinsztein, D.C., 2008. Loss of PINK1 function affects development and results in neurodegeneration in zebrafish. J. Neurosci. 28, 8199–8207.

Blum, D., Torch, S., Lambeng, N., Nissou, M., Benabid, A.L., Sadoul, R., Verna, J.M., 2001. Molecular pathways involved in the neurotoxicity of 6-OHDA, dopamine and MPTP: contribution to the apoptotic theory in Parkinson's disease. Prog. Neurobiol. 65, 135–172.

Clark, I.E., Dodson, M.W., Jiang, C., Cao, J.H., Huh, J.R., Seol, J.H., Yoo, S.J., Hay, B.A., Guo, M., 2006. *Drosophila* pink1 is required for mitochondrial function and interacts genetically with parkin. Nature 441, 1162–1166.

Cook, M.C., Vinuesa, C.G., Goodnow, C.C., 2006. ENU-mutagenesis: insight into immune function and pathology. Curr. Opin. Immunol. 18, 627–633.

Ekker, S.C., Larson, J.D., 2001. Morphant technology in model developmental systems. Genesis 30, 89–93.

Exner, N., Treske, B., Paquet, D., Holmström, K., Schiesling, C., Gispert, S., Carballo-Carbajal, I., Berg, D., Hoepken, H.H., Gasser, T., Krüger, R., Winklhofer, K.F., Vogel, F., Reichert, A.S., Auburger, G., Kahle, P.J., Schmid, B., Haass, C., 2007. Loss-of-function of human PINK1 results in mitochondrial pathology and can be rescued by parkin. J. Neurosci. 27, 12413–12418.

Gandhi, S., Muqit, M.M., Stanyer, L., Healy, D.G., Abou-Sleiman, P.M., Hargreaves, I., Heales, S., Ganguly, M., Parsons, L., Lees, A.J., Latchman, D.S., Holton, J.L., Wood, N.W., Revesz, T., 2006. PINK1 protein in normal human brain and Parkinson's disease. Brain 129, 1720–1731.

Gasser, T., 2005. Genetics of Parkinson's disease. Curr. Opin. Neurol. 18, 363–369.

Haque, M.E., Thomas, K.J., D'Souza, C., Callaghan, S., Kitada, T., Slack, R.S., Fraser, P., Cookson, M.R., Tandon, A., Park, D.S., 2008. Cytoplasmic Pink1 activity protects neurons from dopaminergic neurotoxin MPTP. Proc. Natl. Acad. Sci. U.S.A. 105, 1716–1721.

Hatano, Y., Li, Y., Sato, K., Asakawa, S., Yamamura, Y., Tomiyama, H., Yoshino, H., Asahina, M., Kobayashi, S., Hassin-Baer, S., Lu, C.S., Ng, A.R., Rosales, R.L., Shimizu, N., Toda, T., Mizuno, Y., Hattori, N., 2004. Novel PINK1 mutations in early-onset parkinsonism. Ann. Neurol. 56, 424–427.

Hedrich, K., Hagenah, J., Djarmati, A., Hiller, A., Lohnau, T., Lasek, K., Grünewald, A., Hilker, R., Steinlechner, S., Boston, H., Kock, N., Schneider-Gold, C., Kress, W., Siebner, H., Binkofski, F., Lencer, R., Münchau, A., Klein, C., 2006. Clinical spectrum of homozygous and heterozygous PINK1 mutations in a large German family with Parkinson disease: role of a single hit? Arch. Neurol. 63, 833–838.

Kitada, T., Asakawa, S., Hattori, N., Matsumine, H., Yamamura, Y., Minoshima, S., Yokochi, M., Mizuno, Y., Shimizu, N., 1998. Mutations in the parkin gene cause autosomal recessive juvenile parkinsonism. Nature 392, 605–608.

Kitada, T., Pisani, A., Porter, D.R., Yamaguchi, H., Tscherter, A., Martella, G., Bonsi, P., Zhang, C., Pothos, E.N., Shen, J., 2007. Impaired dopamine release and synaptic plasticity in the striatum of PINK1-deficient mice. Proc. Natl. Acad. Sci. U.S.A. 104, 11441–11446.

Matsui, H., Taniguchi, Y., Inoue, H., Uemura, K., Takeda, S., Takahashi, R., 2009. A chemical neurotoxin, MPTP induces Parkinson's disease like phenotype, movement disorders and persistent loss of dopamine neurons in the medaka fish (*Oryzias latipes*). Neurosci. Res. 65, 263–271.

Park, J., Lee, S.B., Lee, S., Kim, Y., Song, S., Kim, S., Bae, E., Kim, J., Shong, M., Kim, J.M., Chung, J., 2006. Mitochondrial dysfunction in Drosophila PINK1 mutants is complemented by parkin. Nature 441, 1157–1161.

Pridgeon, J.W., Olzmann, J.A., Chin, L.S., Li, L., 2007. PINK1 protects against oxidative stress by phosphorylating mitochondrial chaperone TRAP1. PLoS Biol. 19, e172.

Sim, C.H., Lio, D.S., Mok, S.S., Masters, C.L., Hill, A.F., Culvenor, J.G., Cheng, H.C., 2006. C-terminal truncation and Parkinson's disease-associated mutations down-regulate the protein serine/threonine kinase activity of PTEN-induced kinase-1. Hum. Mol. Genet. 15, 3251–3262.

Tan, E.K., Yew, K., Chua, E., Puvan, K., Shen, H., Lee, E., Puong, K.Y., Zhao, Y., Pavanni, R., Wong, M.C., Jamora, D., de Silva, D., Moe, K.T., Woon, F.P., Yuen, Y., Tan, L., 2006. PINK1 mutations in sporadic early-onset Parkinson's disease. Mov. Disord. 21, 789–793.

Taniguchi, Y., Takeda, S., Furutani-Seiki, M., Kamei, Y., Todo, T., Sasado, T., Deguchi, T., Kondoh, H., Mudde, J., Yamazoe, M., Hidaka, M., Mitani, H., Toyoda, A., Sakaki, Y., Plasterk, R.H., Cuppen, E., 2006. Generation of medaka gene knockout models by target-selected mutagenesis. Genome Biol. 7, R116.

Taymans, J.M., Van den Haute, C., Baekelandt, V., 2006. Distribution of PINK1 and LRRK2 in rat and mouse brain. J. Neurochem. 98, 951–961.

Unoki, M., Nakamura, Y., 2001. Growth-suppressive effects of BPOZ and EGR2, two genes involved in the PTEN signaling pathway. Oncogene 20, 4457–4465.

Valente, E.M., Abou-Sleiman, P.M., Caputo, V., Muqit, M.M., Harvey, K., Gispert, S., Ali, Z., Del Turco, D., Bentivoglio, A.R., Healy, D.G., Albanese, A., Nussbaum, R., González-Maldonado, R., Deller, T., Salvi, S., Cortelli, P., Gilks, W.P., Latchman, D.S., Harvey, R.J., Dallapiccola, B., Auburger, G., Wood, N.W., 2004. Hereditary early-onset Parkinson's disease caused by mutations in PINK1. Science 304, 1158–1160.

Wood-Kaczmar, A., Gandhi, S., Yao, Z., Abramov, A.S., Miljan, E.A., Keen, G., Stanyer, L., Hargreaves, I., Klupsch, K., Deas, E., Downward, J., Mansfield, L., Jat, P., Taylor, J., Heales, S., Duchen, M.R., Latchman, D., Tabrizi, S.J., Wood, N.W., 2008. PINK1 is necessary for long term survival and mitochondrial function in human dopaminergic neurons. PLoS ONE 3, e2455.

Yang, Y., Gehrke, S., Imai, Y., Huang, Z., Ouyang, Y., Wang, J.W., Yang, L., Beal, M.F., Vogel, H., Lu, B., 2006. Mitochondrial pathology and muscle and dopaminergic neuron degeneration caused by inactivation of *Drosophila* Pink1 is rescued by parkin. Proc. Natl. Acad. Sci. U.S.A. 103, 10793–10798.

Zhou, H., Falkenburger, B.H., Schulz, J.B., Tieu, K., Xu, Z., Xia, X.G., 2007. Silencing of the Pink1 gene expression by conditional RNAi does not induce dopaminergic neuron death in mice. Int. J. Biol. Sci. 3, 242–250.

Neuroscience Research 65 (2009) 263–271

Contents lists available at ScienceDirect

Neuroscience Research

journal homepage: www.elsevier.com/locate/neures

A chemical neurotoxin, MPTP induces Parkinson's disease like phenotype, movement disorders and persistent loss of dopamine neurons in medaka fish

Hideaki Matsui [a,c], Yoshihito Taniguchi [b,c], Haruhisa Inoue [a,c], Kengo Uemura [a,c], Shunichi Takeda [b,c,*], Ryosuke Takahashi [a,c,**]

[a] Department of Neurology, Kyoto University, Graduate School of Medicine, Kyoto 606-8507, Japan
[b] Department of Radiation Genetics, Kyoto University, Graduate School of Medicine, Kyoto 606-8501, Japan
[c] Core Research for Evolutional Science and Technology (CREST), Japan Science and Technology Agency, Japan

ARTICLE INFO

Article history:
Received 16 May 2009
Received in revised form 25 June 2009
Accepted 30 July 2009
Available online 7 August 2009

Keywords:
Parkinson's disease
MPTP
Medaka (*Oryzias latipes*)
Movement disorder
Dopamine
Tyrosine hydroxylase

ABSTRACT

Parkinson's disease (PD) is the second most common neurodegenerative disease associated with the degeneration of dopaminergic neurons in the substantia nigra. To create a new model of PD, we used medaka (*Oryzias latipes*), a small teleost that has been used in genetics and environmental biology. We identified tyrosine hydroxylase (TH) immunopositive dopaminergic and noradrenergic fibers and neurons in the medaka brain. Following establishment of a method for counting the number of dopaminergic neurons and an assay for the evaluation of the medaka behavior, we exposed medaka to 1-methyl-4-phenyl-1,2,3,4-tetrahydropyridine (MPTP). The treatment of medaka at the larval stage, but not at adult stage, decreased the number of dopaminergic cells in the diencephalon and reduced spontaneous movement, which is reminiscent of human PD patients and other MPTP-induced animal PD models. Among TH^+ neurons in the medaka brain, only a specific cluster in the paraventricular area of the middle diencephalon was vulnerable to MPTP toxicity. Detailed examinations of medaka transiently exposed to MPTP at the larval stage revealed that the number of dopaminergic cells was not fully recovered at their adult stage. Moreover, the amounts of dopamine persistently decreased in the brain of these MPTP-treated fish. MPTP-treated medaka is valuable for modeling human PD.

1. Introduction

Parkinson's disease (PD) is characterized by the late-onset degeneration of dopaminergic neurons in a subset of neuronal populations represented by the substantia nigra pars compacta in the midbrain. A small proportion of PD is caused by genetic disorder, which provides invaluable insights into the pathogenesis of sporadic PD (Gasser, 2005). Familial PD is caused by autosomal dominant mutations in the genes encoding *α-synuclein* (Polymeropoulos et al., 1997) and *LRRK2* (Paisán-Ruíz et al., 2004; Zimprich et al., 2004), while juvenile parkinsonism is associated with recessive mutations in the genes encoding *parkin* (Kitada et al., 1998), *DJ-1* (Bonifati et al., 2003), and *PINK1* (Rogaeva et al., 2004; Valente et al., 2004). Various models have been developed in several species in order to understand the mechanisms underlying the pathogenesis of PD, including mouse (Bové et al., 2005; Fleming et al., 2005), *Drosophila* (Cauchi and van den Heuvel, 2006), *Caenorhabditis elegans* (van Ham et al., 2008) and yeasts (Outeiro and Lindquist, 2003). However, the pathogenesis of PD remains largely unknown.

Small laboratory fish such as zebrafish (*Danio rerio*) and Japanese medaka (*Oryzias latipes*) are attractive vertebrate animal models, because they are easy to handle and produce large numbers of progeny per generation (Wittbrodt et al., 2002). Medaka is a small aqueous fish that inhabits Asia and has been used as a model organism since early 1900s (Aida, 1921). It has several advantages over zebrafish or goldfish in modeling PD. First, the whole genome has been sequenced and assembled since the size of medaka genome is only 700 Mb, half the size of the zebrafish genome (Kasahara et al., 2007). Second, several inbred strains have been established in medaka, but not in zebrafish. The lack of genetic variations among individuals may simplify and facilitate genetic studies, and is particularly important for disease models. The goldfish is not suitable for genetic research because it does not have good genetic information nor technology for genetics, while most techniques that are used for zebrafish studies are applicable to medaka. Third, the body of medaka is more transparent than

* Corresponding author at: Department of Radiation Genetics, Kyoto University, Graduate School of Medicine, Yoshida-Konoe-cho, Sakyo-ku, Kyoto 606-8501, Japan. Tel.: +81 75 753 4410; fax: +81 75 753 4419.
** Corresponding author at: Department of Neurology, Kyoto University, Graduate School of Medicine, 54 Shogoin-Kawahara-cho, Sakyo-ku, Kyoto 606-8507, Japan. Tel.: +81 75 751 3770; fax: +81 75 751 9780.
E-mail addresses: stakeda@rg.med.kyoto-u.ac.jp (S. Takeda), ryosuket@kuhp.kyoto-u.ac.jp (R. Takahashi).

0168-0102/$ – see front matter © 2009 Elsevier Ireland Ltd and the Japan Neuroscience Society. All rights reserved.
doi:10.1016/j.neures.2009.07.010

that of the zebrafish or goldfish, and it is easy to visualize the *in vivo* target structures. Fourth, cryopreservation of the sperm is easy and reliable, so we can maintain and store numerous strains in the laboratory (Yang and Tiersch, 2009). Finally and most importantly, we have already retrieved PD-related mutants including *parkin* from our TILLING (Targeting Induced Local Lesions IN Genomes) library of medaka (Taniguchi et al., 2006).

1-Methyl-4-phenyl-1,2,3,4-tetrahydropyridine (MPTP) is a neurotoxin that induces PD-like symptoms. It is metabolized in glial cells to 1-methyl-4-phenylpyridinium (MPP^+), and is subsequently incorporated by dopaminergic neurons via dopamine transporter, thereby selectively damaging the dopaminergic neurons through inhibiting the activity of the mitochondria respiratory chain (Gerlach et al., 1991). It has been widely used to generate zebrafish and goldfish model of PD together with other neurotoxins such as 6-hydroxydopamine and rotenone (Pollard et al., 1992; Anichtchik et al., 2004; Wen et al., 2008; Bretaud et al., 2004; Lam et al., 2005; McKinley et al., 2005). However, these studies mainly focus on the acute or subacute effects of neurotoxins on zebrafish or goldfish. One caveat is that the adult neurogenesis occurs extensively in the brain of fish and that neurons are added continuously to various brain regions (Grandel et al., 2006). Therefore, it is important to examine the consequences of MPTP-induced brain lesions over a long period of time in the research using fish. In this study, we report the long-term effect of MPTP on medaka dopaminergic system evaluated by several assays including histological analysis of dopaminergic neurons and the behavioral tests.

2. Materials and methods

2.1. Fish maintenance

Wild-type medaka of *Kyoto-cab* strain was maintained at 27 °C in a recirculating aquaculture system equipped with carbon filtration, ultraviolet light sterilizers and biofiltration. Adult fish were kept under a reproduction regimen (14 h light/10 h dark). Eggs were kept in a dark box at 28 °C.

2.2. MPTP treatment

The MPTP-hydrochloride (Sigma–Aldrich, MO, USA) was dissolved in distilled water to 10 mg/ml. Safety precautions included the use of protective clothing, globes, goggles, masks and decontamination of all surfaces and solutions with 1% bleach at the end of each experiment. For exposure of adult fish, three fish (90-dpf) were kept in 100 ml of water each containing different concentration of MPTP. The water was changed and MPTP was freshly added to the water every week. Three weeks after treatment, the fish was rinsed seven times for total clearance of MPTP and subjected to the analysis (Fig. 2A). For exposure of larvae, five 10-dpf larvae were kept in a cup containing 50 ml water with various concentration of MPTP. Two days after treatment, MPTP was removed and the fish were used for the analysis (Fig. 2B). We used littermates in a series of experiments and all the experiments were done at least twice.

2.3. High performance liquid chromatography

Brain was homogenized in 100 μl of 0.4 M $HClO_4$ containing 4 mM $Na_2S_2O_5$ and 4 mM diethylenetriaminepentaacetic acid. The supernatant by centrifugation at 18,500 × *g* for 5 min was used for measurement of free catechols. High performance liquid chromatography (HPLC) was conducted with a mobile phase containing bufferA:acetonitrile:methanol = 1000:25.9:62.9 (v/v/v) (bufferA: 0.1 M phosphate, 0.05 M citrate, 4 mM sodium 1-heptanesulfonate and 0.1 mM EDTA, pH 3.0). Dopamine and metabolites were detected with series coulometric detector (ESA, Inc., Chelmsford, MA, USA). Data were collected and processed on a CHROMELEON™ Chromatography Data Systems 6.40 (Dionex, Sunnyvale, CA, USA). The pellet was then reserved for the analysis of the protein content. For this purpose, the pellet was solubilized in 100 μl of 0.5 N NaOH at 60 °C and the protein was quantified by the BCA assay method, using bovine serum albumin (BSA) as the standard.

2.4. Immunohistochemistry

After organs were examined under the stereomicroscope, fish were fixed in 4% paraformaldehyde for 24 h and embedded in paraffin. Each brain was sectioned at 20-μm thickness and incubated with mouse anti-tyrosine hydroxylase (TH) antibody (Millipore, MA, USA, 1:500) for 1 h. Immunoperoxidase detection was carried out by using Vector Elite ABC kit with DAB (Vector Laboratories, CA, USA) on every section. The number of dopaminergic neurons in the diencephalon was determined by counting the nucleus of TH^+ neurons in coronal sections using OLYMPUS BX51 microscope with MICROFIRE digital camera (Olympus, Japan) and Stereo Investigator (MBF Bioscience, VT, USA). Photographs were taken by the same equipments. Whole mount immunohistochemistry of larvae was carried out as previously described (Shimamura and Takeichi, 1992). Mouse anti-TH antibody (Millipore, MA, USA, 1:100) was detected via fluorescence using anti-mouse IgG conjugated with Alexa Fluor 546 (Invitrogen, WI, USA). Images were acquired by LSM510 microscope (Carl Zeiss, Germany) and subjected to quantitative analysis using Photoshop (Adobe, CA, USA).

2.5. Western blotting

Brains were homogenized in RIPA buffer (25 mM Tris–HCl pH 7.6, 150 mM NaCl, 1% NP-40, 1% sodium deoxycholate, 0.1% SDS) with protease inhibitors and processed for SDS-PAGE. Immunoreactive bands were detected with ECL reagent or ECL plus reagent (GE Healthcare Life Sciences, Japan) and chemiluminescent signal was visualized by the exposing membrane to Fuji RX-U X-ray film (Fuji Film, Japan). Films were scanned and densitometric analysis of blots was performed using ImageJ software (National Institute of Health). The background intensity of the film was subtracted from the band intensity. Anti-TH monoclonal antibody (1:1000, mouse anti-TH, MAB318, Millipore) was used for the western blotting analysis of TH. For the loading control, anti-β-actin monoclonal antibody (1:5000, AC-15, Sigma–Aldrich) was used.

2.6. Behavioral analysis

Fish were subjected to a spontaneous swimming measuring test during a light phase. Images were collected by a video camera positioned above the water tank under a low indirect dimly white light, and analyzed by a computer-assisted system (Muromachi Kikai, Japan). The water tank was a transparent circular field (2 cm water depth, 27 °C) with the diameter of 5 cm for larvae and 20 cm for adults. We started to acquire the images 1 min after the larvae was entered into the water tank. Adult medaka is more wary of environmental changes compared to zebrafish and larval medaka, and they tend to remain stationary when put in a new tank. We started to acquire the images 1 min after the adult fish began to move in a new water tank. Beginning of this movement was automatically defined when fish moved from one section to another section (Fig. 5D). The data were collected for 1 or 5 min for larvae and adults, respectively. The larvae and adults were judged as they were swimming only when the moving speed exceeded 0.025 cm/0.1 s and 0.1 cm/0.1 s, respectively. Total swimming distance, frequency of swimming movement (duration of swimming movement divided by the total time of observation), and swimming velocity (total swimming distance divided by duration of swimming movement) were measured and compared among the groups.

2.7. Statistical analysis

Data were expressed as mean ± standard error of the mean (SEM). The results were statistically evaluated for significance by applying ANOVA with post hoc analysis using Dunnett's test. Differences were considered significant when $p < 0.05$.

3. Results

3.1. Distribution of dopaminergic neurons in the brain of adult medaka

To examine the distribution of dopaminergic neurons in medaka brain, we used immunohistochemistry of TH to visualize dopaminergic neurons. We identified TH immunopositive (TH^+) fibers in the telencephalon (Fig. 1B). This TH^+ structure in the teleost brain is relevant to the striatum in the human brain (Rink and Wullimann, 2004). Medaka TH^+ neurons aligned from the telencephalon to the diencephalon along the ventro-medial side of the brain (Fig. 1C–F). In the rostral part of diencephalon, clusters of small neurons were found in both dorsal and ventral areas (Fig. 1D). Large TH^+ neurons were distributed towards the caudal area around the ventricle in the middle diencephalon (Fig. 1E). The rostro-ventral TH cluster was around the nucleus posterioris periventricularis (NPPv) and the middle one around the NPPv and the nucleus anterior tuberis. At the most caudal part of the diencephalon, there were small neurons on the dorsal side (Fig. 1F). This cluster existed around the nucleus posterior thalami. We could easily distinguish these clusters because the size of neurons

in each cluster was different and these clusters were clearly separated anatomically from each other. We also detected TH^+ noradrenergic neurons in the medulla oblongata (Fig. 1G).

The distribution of TH^+ neurons in the medaka diencephalon largely matched with previously published data on zebrafish TH^+ neurons and medaka neurons that exhibit *Nurr1* mRNA (Rink and Wullimann, 2004; Kapsimali et al., 2001). Histological examination using retrograde tracers suggests that a subset of dopaminergic neurons in the diencephalon of zebrafish project to the striatum-like structure and may be equivalents of the substantia nigra neurons in mammals (Rink and Wullimann, 2004). For the subsequent experiments in this study, we counted only the number of dopaminergic neurons in the diencephalic clusters because these will contain an equivalent of the substantia nigra. TH^+ neurons in the middle diencephalon show a distinct morphology with the large cell body and the intense cytoplasmic staining hollowed by a clear nucleus (Supplementary Fig. 1). There are 87.5 ± 5.6 ($n = 8$) of such cells in around 200 μm in the paraventriclular area of the middle diencephalon (Fig. 3C). In the rostral and caudal regions to this area, we found 145.9 ± 9.1 and 81.9 ± 8.0 TH^+ neurons, respectively, with a smaller cell body (Fig. 3C). Counting these cells yielded highly reproducible data. We also counted the number of TH^+ neurons

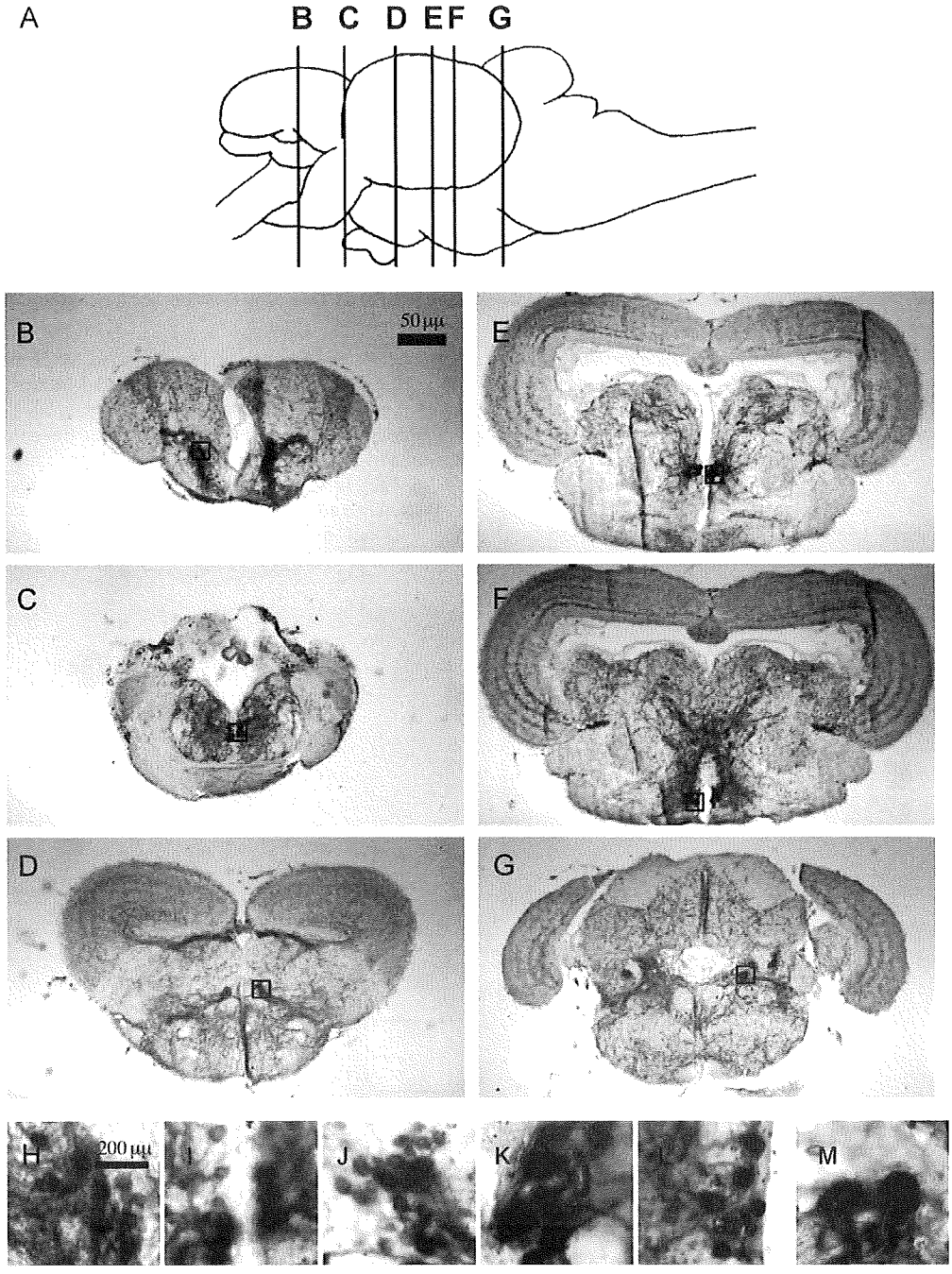

Fig. 1. The distribution of TH^+ neurons in adult medaka diencephalon and medulla oblongata. Coronal sections at different rostro-caudal levels show the localization of TH^+ dopaminergic fibers and neurons in the telencephalon (B), preoptic area (C) and diencephalon (D: rostral, E: middle, F: caudal). TH^+ neurons were also distributed in the medulla oblongata (G). Insets (H–M) are the magnified picture of original images (B–G) respectively. The positions of each section are illustrated by vertical lines in (A).

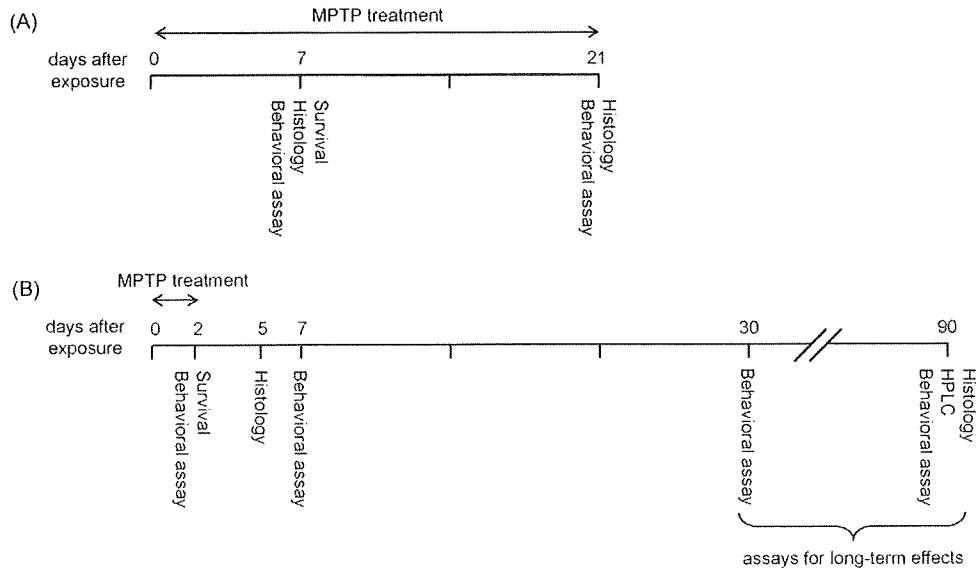

Fig. 2. MPTP treatment schedule. (A) For 3 weeks exposure to adult fish. 90-dpf fish were exposed to MPTP. MPTP was removed 21 days after the first exposure (111-dpf) and the brains of these fish were immediately fixed for histology. (B) For 2 days exposure to larvae. 10-dpf fish were exposed to MPTP. MPTP was removed 2 days after the first exposure (12-dpf). Assays including HPLC, behavioral analysis and histology were done at the indicated time course. The numbers indicate the days after the first exposure to MPTP.

(43.8 ± 4.2) in the medulla oblongata to monitor the effect of MPTP on noradrenergic neurons. In summary, we identified several clusters of TH^+ neurons in medaka brain and established a reliable method for evaluating the number of dopaminergic neurons.

3.2. *Short-term effect of MPTP on adult and larval medaka*

Several studies have been reported regarding the cytotoxic effect of MPTP on zebrafish and goldfish. In order to investigate the interspecies differences of sensitivity to MPTP between medaka and other model teleost fish, we treated 3 months old and 10-dpf (days post-fertilization) medaka with varying concentration of MPTP for 1 week (Fig. 2A). The embryonic development is slow in medaka in comparison to zebrafish, and it usually takes 7–10 days for medaka larvae before hatching out of the eggshell.

When the adult fish were exposed to 0.1 μg/ml of MPTP, all the fish (10 out of 10) survived a-week-long treatment, whereas 0.2 μg/ml of MPTP was tolerated by only a small fraction of fish (2

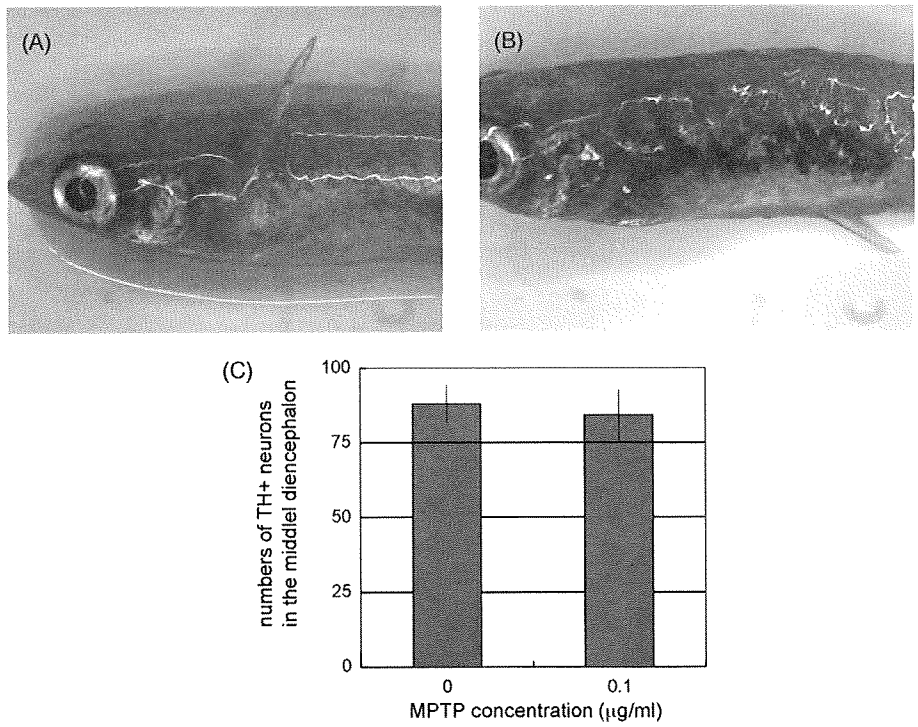

Fig. 3. Features of fish exposed to MPTP at the adult stage. (A and B) Skin images of control fish (A) and MPTP-treated fish (B). The skin was darkened by MPTP treatment (white allow). (C) The numbers of TH^+ neurons in the middle diencephalon. There was no significant reduction in the TH^+ neurons of MPTP-treated fish. $n = 8$ for each group.

out of 10). Following the treatment with 0.1 μg/ml of MPTP, the skin became darkly pigmented as in the MPTP-treated zebrafish (Fig. 3A and B), presumably due to the impairment of peripheral catecholaminergic nerves (Bretaud et al., 2004). However there was no significant decrease in the number of TH^+ cells in the diencephalon and medulla oblongata, nor in the level of spontaneous swimming movement of the MPTP-treated adult medaka at 0.1 μg/ml (data not shown). Prolonged exposure of up to 3 weeks also did not alter the number of TH^+ neurons nor the spontaneous movement (Fig. 3C, data not shown).

Next, we sought to determine the effect of MPTP on medaka larvae since higher sensitivity of TH^+ neurons to MPTP has been reported in zebrafish larvae compared to the adult (McKinley et al., 2005). When medaka larvae were treated with 0.2 μg/ml of MPTP for 2 days, 35 out of 50 (70%) fish survived, while only 1 out 10 (10%) survived after the treatment with 0.3 μg/ml of MPTP. The cytotoxic effect of MPTP on dopaminergic neurons in larvae was then determined by the whole mount immunohistochemistry 3 days after the end of exposure to 0.2 μg/ml of MPTP. In contrast to the fish exposed to MPTP at the adult stage, the TH^+ signal in the diencephalon was markedly decreased in the fish exposed to MPTP at the larval stage (Fig. 4C). The quantitative analysis showed 84% decrease in the TH^+ signal in the MPTP-treated fish compared to the non-treated control (Fig. 4E). These results indicate that the MPTP elicits the reduction of TH^+ neurons in medaka larvae, but not in the adult fish.

Since the histological analysis showed that MPTP impaired dopaminergic neurons, we monitored the spontaneous swimming movement of larvae exposed to 0.2 μg/ml of MPTP using the automated tracking system. Starting immediately after the end of exposure, MPTP-treated fish showed marked decrease in the total swimming distance (Fig. 5A). Additionally, the MPTP treatment significantly diminished the frequency and velocity of swimming (Fig. 5B and C). Although 0.2 μg/ml of MPTP is much lower than the concentration used in previous reports in zebrafish (5–45 μg/ml) (McKinley et al., 2005; Wen et al., 2008; Bretaud et al., 2004), even lower concentration of MPTP (0.02 μg/ml) showed the reduction in both the number of TH^+ neurons and the spontaneous movement (Fig. 5A–D). The group treated with 0.02 μg/ml of MPTP exhibited the intermediate phenotype between the control and the group treated with 0.2 μg/ml of MPTP, suggesting the dose–response relationship. To exclude the possibility of symptoms other than PD, we forced the fish to swim by giving them a touch or sound stimulus. We found that MPTP-treated fish and their untreated controls displayed comparable quick response to these stimuli (data not shown), suggesting that MPTP affects the spontaneous movement of medaka without associating with muscle weakness, paralysis and sensory defect.

3.3. *Persistent loss of dopaminergic neurons in the brain of medaka exposed to MPTP at the larval stage*

Not a few studies have revealed the cytotoxic effect of MPTP on TH^+ cells in teleost fish (Pollard et al., 1992; Anichtchik et al., 2004; Wen et al., 2008; Bretaud et al., 2004; Lam et al., 2005; McKinley

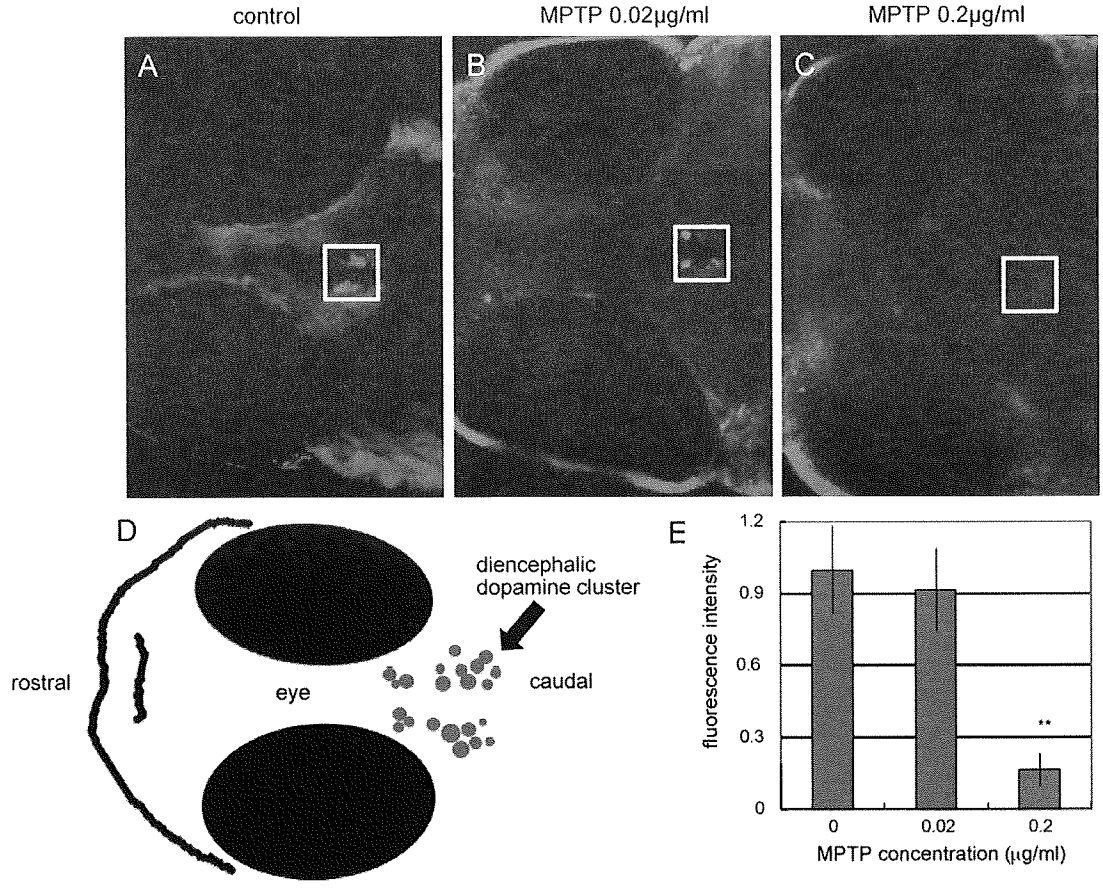

Fig. 4. Whole mount TH staining of medaka larvae following exposure to MPTP. White squares indicated diencephalic dopamine neurons. Images were taken 5 days after the first exposure (15-dpf) (A: control, B: MPTP 0.02 μg/ml and C: MPTP 0.2 μg/ml), and were used quantitative analysis. (D) Showed simple atlas of the images. (E) Quantitative comparisons of the fluorescence of TH^+ neurons. The region of interest was set as a minimal square including TH^+ neurons in the diencephalon. 0.2 μg/ml MPTP treatment markedly reduced TH^+ signals in the diencephalon (C and E). $^{**}p < 0.01$ vs. control. $n = 4$ for each group.